Sedimentologika

Research article

Source-to-sink controls on modern fluvial sands in the Pantanal back-bulge basin (Brazil)

Edward L. Lo[1*], Aguinaldo Silva[2], Sidney Kuerten[3], Rômullo O. Louzada[4], Giliane G. Rasbold[1], Michael M. McGlue[1]

[1] Department of Earth and Environmental Sciences, University of Kentucky, Lexington, KY, USA
[2] Câmpus do Pantanal, Universidade Federal de Mato Grosso do Sul, Corumbá, Brazil
[3] Unidade Universitária de Jardim, Universidade Estadual de Mato Grosso do Sul, Jardim, Brazil
[4] Cidade Universitária, Universidade Federal de Mato Grosso do Sul, Campo Grande, Brazil

*corresponding author: Edward L. Lo (edward.lo@uky.edu)

doi:10.57035/journals/sdk.2023.e11.1152

Editors: Ian Kane and Brian Burnham
Reviewers: Eduardo Garzanti and Ian Kane
Copyediting, layout and production: Romain Vaucher, Farid Saleh, Gabriel Bertolini and Faizan Sabir

Submitted: 05.04.2023
Accepted: 16.08.2023
Published: 12.09.2023

Abstract | Sedimentological processes are underexplored in retro-arc basin segments of source-to-sink systems, particularly in the distal back-bulge depozone. The extant Pantanal Basin of Latin America is a large sub-tropical continental back-bulge for which the boundary conditions on riverine sedimentation (tectonics, climate, phytogeography) are reasonably understood. Here, we use a new database of riverbed sand samples (n = 97) to investigate the modern provenance of the Pantanal Basin. Petrographic analysis of grain-mounted thin sections and Gazzi-Dickinson point counting were used to assess the framework composition of the sands, and a pour point analysis based on geographic information systems (GIS) defined the hinterland geological environment for each sample. Six provenance domains were defined: (a) lowlands, (b) Amazon craton, (c) Rio Apa craton, (d) plateau, (e) South Paraguay Belt, and (f) North Paraguay Belt. Most Pantanal samples are quartzose non-orogenic detritus (Qt88\F5\L7). Rivers draining the Paraguay Belt highlands carry more lithic grains derived from carbonate parent rocks. The occurrence of plagioclase grains is rare. However, river sands where >30% of the total assemblage was K-feldspar were present downstream of foliated metamorphic outcrops of the Rio Apa craton. Sand relatively rich in fine K-feldspar grains in the medial Taquari River megafan were attributed to channel avulsion, incision, and reworking of floodplain deposits. Statistical analysis suggests that bedrock lithology and average annual rainfall are important controls on fluvial sands in the Pantanal Basin, with watershed slope, temperature, and dilution playing secondary roles in the spatial distribution of dominant grain types. This study provides new actualistic data that aim to improve interpretations of the geological record.

Resumo | Os processos sedimentológicos nos segmentos entre a área fonte e deposição são poucos explorados em bacias de retroarco, particularmente em zonas de deposição distais da região de *back-bulge*. A Bacia do Pantanal, na América Latina, é uma vasta região de *back-bulge* continental e clima sub-tropical, em que as condições regionais de contorno para a sedimentação fluvial (tectonismo, clima e fitogeografia) estão razoavelmente entendidas. Neste estudo, utilizamos amostras de areia do leito de rios (n = 97) para investigar a proveniência moderna de sedimentos da Bacia do Pantanal. A análise petrográfica dos grãos montados em lâminas petrográficas e a contagem modal através do método de Gazzi-Dickinson foram usadas para avaliar a composição estrutural das areias, e uma análise do ponto de drenagem baseada em sistemas de informação geográfica (SIG) definiu o ambiente geológico de origem para cada amostra. Foram definidos seis domínios de proveniência: (a) várzea, (b) Cráton Amazônico, (c) Cráton Rio Apa, (d) Planalto, (e) Faixa Paraguai Sul, e (f) Faixa Paraguai Norte. A maioria das amostras apresentou detritos não-orogênicos quartzosos (Qt88\F5\L7). Os rios que drenam as terras altas da Faixa Paraguai carregam mais grãos líticos derivados de rochas-mãe carbonáticas. A ocorrência de plagioclásio foi rara, mas as areias dos rios com >30% da assembleia total em K-feldspato estavam presentes à jusante dos afloramentos metamórficos foliados do Cráton Rio Apa. As areias relativamente ricas em grãos finos de K-feldspato foram atribuídas à avulsões do canal, bem como a incisão e exposição de depósitos de várzea na porção média do megaleque do rio Taquari. A análise estatística sugere que a litologia e a precipitação média anual são importantes controles sobre as areias fluviais na Bacia do Pantanal, enquanto a inclinação da bacia hidrográfica, temperatura e diluição desempenham papéis secundários na distribuição espacial dos tipos de grãos predominantes. Este estudo fornece novos dados atuais que visam aprimorar as interpretações do registro geológico.

Lay summary | Sediment generation and transport processes are not fully understood in sedimentary basins far from mountain belts. We collected 97 sand samples from rivers in the Pantanal Basin (Brazil) and evaluated 500 grains in each sample for composition using grain mount thin sections. Most sands were rich in quartz. The type of lithic grains and feldspar content varied with sediment source characteristics. Statistical analysis suggests that parent rock and mean annual precipitation were the main controls on sand composition. The slope, temperature, and dilution were secondary influences on the sand mineralogy. This information can help improve our understanding of paleodepositional deposits.

Keywords: Back-bulge basin, Fluvial sediment, Pantanal, Provenance, Tropical wetlands

1. Introduction

Modern provenance studies have examined river sands from several areas of the Andean foreland basin, particularly in the wedgetop and foredeep depozones (Johnsson, 1990; Savage & Potter, 1991; Johnsson et al., 1991; McGlue et al., 2016; Capaldi et al., 2019). Much of the Andean provenance research has focused on individual drainages or sets of major tributaries, whereas basin-scale studies are less common (Garzanti et al., 2006, 2014, 2021a, 2022). The existing modern sand provenance database from Latin America has been used to characterize the influence of collisional mountain building on sediment generation near the thrust front, which has proven valuable for calibrating tectono-stratigraphic models and interpreting mountain building processes and timelines from the ancient sedimentary record (Carrapa et al., 2011; McGlue et al., 2016; Tineo, 2020; Papa et al., 2021; Garzanti et al., 2021a). Since the recognition of ancient forebulge and back-bulge deposits in the rock record is often crucial for establishing the history of orogenesis and flexural basin development, petrographic data from modern rivers in these depozones provide the potential for improving paleoenvironmental interpretations. However, this data is rare for the distal depozones of the Andean foreland. Consequently, the processes that influence sediment generation, transport, storage, and deposition are poorly known. Here, we provide the first comprehensive description of sand composition in a modern back-bulge basin, using the Pantanal Basin and its rivers as the focus.

The purpose of this study is to describe the composition of modern river sediments collected from a broad spatial network of stations in the Pantanal Basin of western Brazil (Figure 1). The Cenozoic Pantanal Basin is the back-bulge depozone of the central Andean retro-arc basin (DeCelles & Giles, 1996; Horton & DeCelles, 1997; Horton, 2022). Known for its strongly seasonal flood pulse that aid to form one of the largest and most biodiverse tropical wetland systems in the world, the Pantanal remains understudied from a sedimentary geology perspective, and the source-to-sink processes of sediment generation, transport, and deposition remain largely unexplored (Assine et al., 2016). Like many continental back-bulges, the Pantanal is dominated by low-gradient meandering rivers, vast megafan floodplains, shallow lakes, and heavily vegetated swamps (Assine et al., 2015). The Pantanal forms the headwaters of the Paraguay River. The Upper Paraguay River flows from north to south along the basin's western margin and sets the regional base level. Numerous lateral drainages, including several that form large and prominent distributive fluvial systems such as the Taquari, Paraguay, and Cuiabá megafans (Assine & Silva, 2009; Zani et al., 2012; Pupim et al., 2017), run into the Pantanal Basin from northern and eastern plateaus. The plateaus are regionally known as *planalto*, which was formed from erosion of Paraná Basin rocks prior to final basin development (Assine et al., 2016). Regarding Andean tectonics, the Pantanal lies between a broad flexural forebulge that is dominantly covered by alluvium and the Brazilian craton (Chase et al., 2009; McGlue et al., 2016). Drainages flowing east across the low-amplitude forebulge appear to have a low sediment contribution to the Pantanal Basin, due to the topographic barrier imposed by the Amazon craton (Kuerten & Stevaux, 2021). Therefore, rivers draining the craton, as well as the Paraguay River itself, dominate with respect to sand delivery to the Pantanal.

Relatively diverse bedrock characterizes the hinterland of the Pantanal Basin today, whereas the conditions that influence weathering such as temperature and precipitation gradients are more muted. We therefore hypothesize that geological characteristics, in particular parent lithology, control river sand composition in this basin. Provenance lithotypes have been shown to determine the composition and texture of the sand-sized fraction across diverse climatic and tectonic environments (Heins, 1993; Heins & Kairo, 2007). We employed optical petrographic analysis and Gazzi-Dickinson point counts on a database of river sand samples that were tied to hinterland lithology using geographic information systems (GIS) to test this hypothesis.

2. Geological setting

The name *Pantanal* is derived from the Portuguese words *pântano* (meaning wetland or swamp) and the suffix *-al* (meaning abundance, agglomeration, or collection). The lowlands are ~150,000 km^2 but the watershed known as the Upper Paraguay River Basin spans ~465,000 km^2 across Brazil, Bolivia, and Paraguay (Paz et al., 2010; Bravo et al., 2012). The Pantanal is a Cenozoic-age basin that has accumulated ~500 m of sediment (Horton & DeCelles, 1997; Ussami et al., 1999). The basin formed from the flexure of the continental crust in response to the Andean orogeny (Horton & DeCelles, 1997; Assine, 2005; Assine

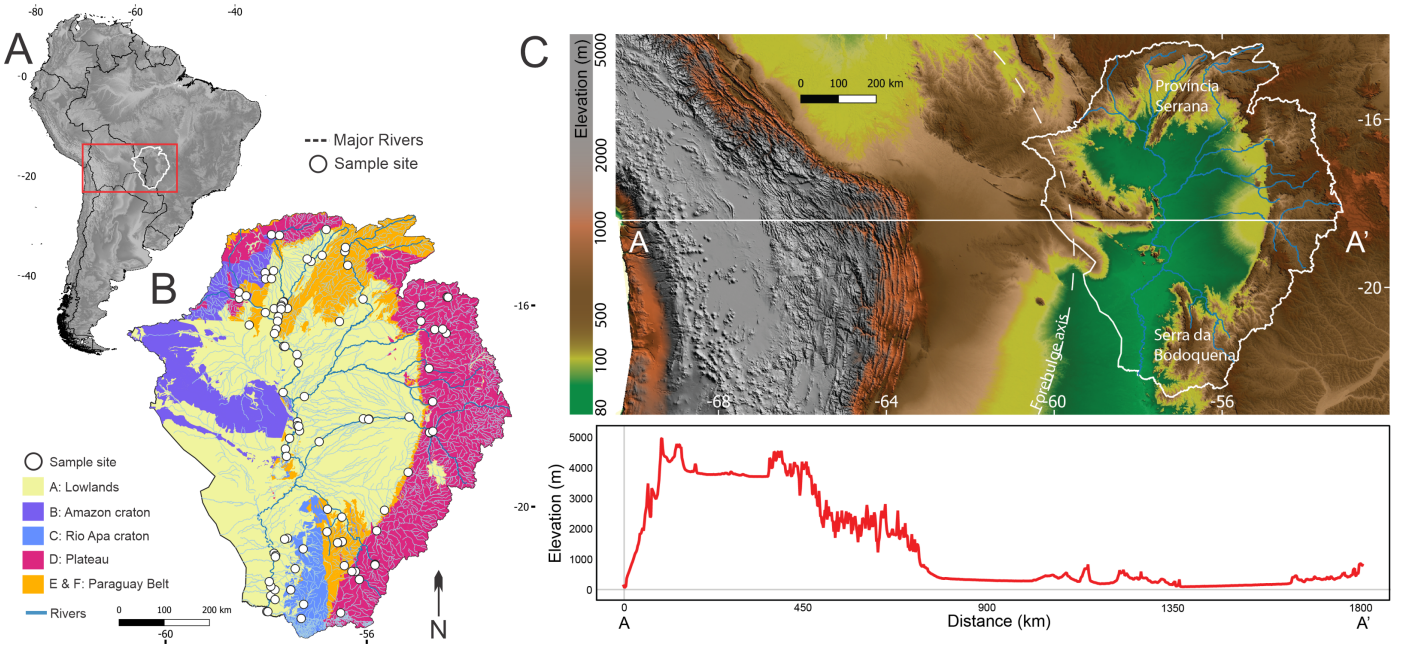

Figure 1 | (A) Upper Paraguay River Basin (white outline) in South America with major rivers (blue lines). (B) Pantanal Basin sediment generation (provenance) regions with hydrologic map, referenced throughout the text. Much of the areas covered at the surface by wetlands are designated as lowlands, in contrast with the fringing cratons and the plateau. C) GTOPO30 digital elevation model of South America (USGS, 1996), including a simplified topographic cross-section A-A' from Google Earth©. The forebulge axis and the Província Serrana and Serra da Bodoquena mountain ranges are labeled.

et al., 2016). The crust is thin, ranging from 38-43 km on the west and thinning to <35 km on the eastern margin of the basin (Rivadeneyra-Vera et al., 2019; Cedraz et al., 2020; Shirzad et al., 2020). The Pantanal has been a site of intraplate seismicity, with notably large earthquakes in 1964 and 2009 (Dias et al., 2016). The Transbrasiliano lineament runs NE-SW along the southeastern flank of the basin, but seismic events have not been explicitly related to reverse or strike-slip motion on this structure.

In the context of fluvial sediment transport, the Upper Paraguay River Basin watershed extends eastward from the Andean forebulge (Bravo et al., 2012). Within the Upper Paraguay River Basin in Brazil, the point of highest elevation is in the plateau at 1260 m above sea level (m.a.s.l.), and the lowest point is at 70 m.a.s.l. near the Pantanal Basin outlet at the confluence of the Apa River and Paraguay River (Figure 1). The average watershed slope is greatest at the transition out of the plateau, but within the lowlands, the slope is much reduced (Zani et al., 2012).

We consider the Pantanal to be supplied with sediment from six distinct provenance regions (Figure 1B). The Pantanal is bounded by the Amazon craton in the northwest and consists of the Sunsás and Rondônia-San Ignacio provinces with granites, granodiorites, schists, and dikes of quartz-diorite and quartz-gabbro composition (Rizzotto & Hartmann, 2012; Horbe et al., 2013; Braga et al., 2019). The southwestern Pantanal hosts the Rio Apa craton, consisting of gneisses, granites, granodiorites, amphibolites, schists, and quartzites (RadamBrasil, 1982; Alvarenga et al., 2011). The eastern Pantanal is bounded by the plateau, composed of Phanerozoic sedimentary lithotypes derived from the Paraná Basin (Figure 2B). The South Paraguay Belt hosts phyllites, schists, metarenites, quartzites, and dolomitic and calcitic marble in the Serra da Bodoquena (Figure 1C). The North Paraguay Belt includes the Província Serrana with phyllites, schists, calcitic limestones, siltites, and arenites (RadamBrasil, 1982).

Mean annual rainfall is ~1800 mm in the northern and eastern Pantanal, but it reduces to ~1200 mm along the western and southern margins (Alvares et al., 2013; Marengo et al., 2015; Fick & Hijmans, 2017) (Figure 3B). The hydroclimate of the Pantanal Basin is defined by a distinct wet and dry season; most of the annual rainfall occurs in the months of December, January, and February. The dry season reaches its apex in the months of June, July, and August. The annual migration of the Intertropical Convergence Zone is responsible for this seasonality of precipitation and patterns in floodplain inundation and phytogeography (Ivory et al., 2019). For the Paraguay River, such a precipitation pattern results in a flood pulse effect, which manifests as a several month delay in the peak discharge at the southern end of the basin near its outlet (Junk et al., 2006). The annual temperature range is 21-27°C with a mean value of ~25°C and is described as tropical savanna climate in the Köppen climate system (McGlue et al., 2011). The mean annual precipitation across the basin is ~1444 mm with an average annual temperature of 25°C (Fick & Hijmans, 2017). Overall, the northern Pantanal experiences higher maximum temperature and precipitation than does the southern Pantanal, where evaporation is higher (Figure 3B). The soil and vegetation composition provide important context for understanding the sediment routing system (Figures 2A, 3A). The soils are dominantly planosols in the lowland flooded savanna,

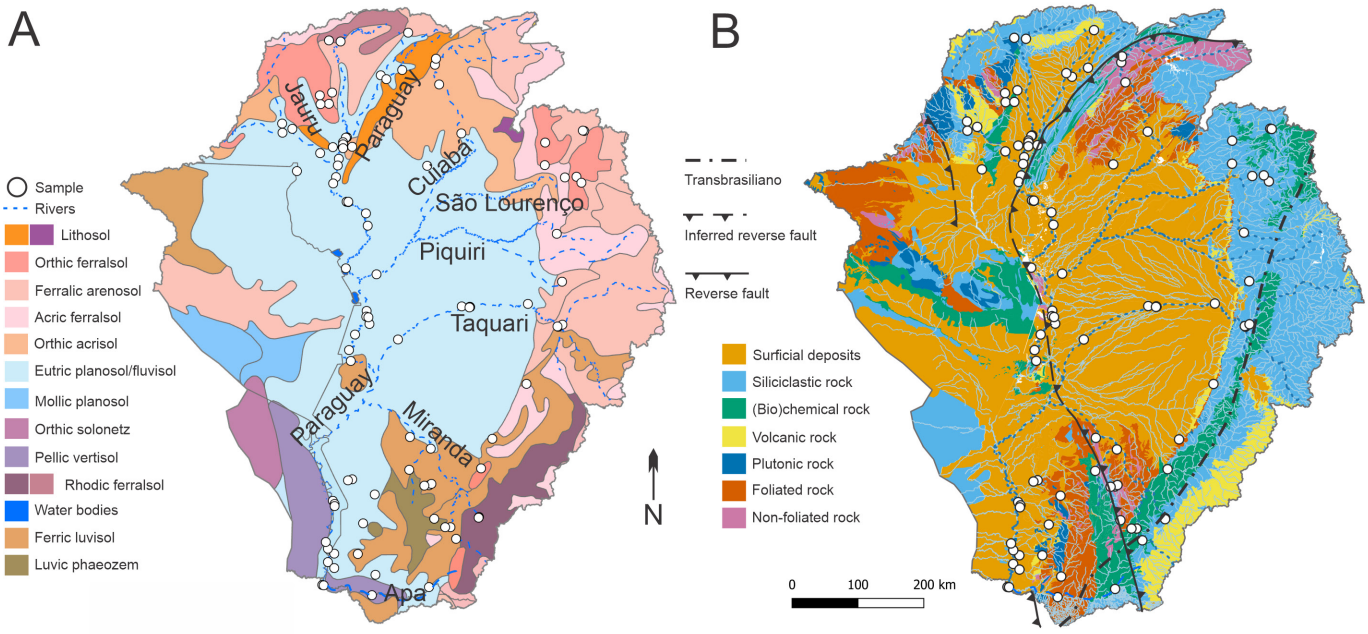

Figure 2 | (A) Soil map for the Pantanal Basin (FAO, 1970). The primary soil classes are eutric planosol/fluvisol (Benedetti et al., 2011). (B) Geology of the Pantanal Basin and drainage network, with major faults in the region. The plateau is dominated by siliciclastic sedimentary rock, whereas metamorphic rocks are restricted to the cratons and Paraguay Belt. Geologic maps were obtained from Bolivia (Dirección de Ordenamiento Territorial, Gobierno Autónomo Departamental de Santa Cruz), Paraguay (Vice Ministerio de Minas y Energía), and Brazil (Serviço Geológico do Brasil, CPRM). Faults were drawn based on published studies (Rizzotto & Hartmann, 2012; Warren et al., 2015; Faleiros et al., 2016; Barboza et al., 2018; Rivadeneyra-Vera et al., 2019; Cedraz et al., 2020).

whereas the *cerrado* region contains mostly ferralsols and arenosols plus luvisols in the southern *cerrado* (Benedetti et al., 2011). Lithosols, planosols, vertisols, and solonetz are present in limited geographic extent in the Pantanal Basin (Figure 2A). Much of the Pantanal consists of flooded savanna and *cerrado* (tropical savanna) environments; dry forest and dry Chaco make up the balance of the basin (Figure 3A). *Cerrado* and dry forest ecotones occupy the hinterland, and flooded savanna occupies the lowlands. Some areas of the basin along the western margin are dry *cerrado*, with minor humid Chaco and Atlantic Forest parts (Figure 3A).

3. Methods

The Pantanal has few urbanized areas, with vast tracts of wilderness that are difficult or impossible to access across large portions of the year. To obtain a preliminary representative sample set, pour point analyses were conducted using GIS to identify viable sampling stations in accessible locations. A pour point is the lowest point in a given watershed to which all of the waters drain, thus defining the area upstream that contributes sediment (Gleyzer et al., 2004). We used Shuttle Radar Topography Mission (SRTM) digital elevation models (DEMs) from the USGS EarthExplorer website (https://earthexplorer.usgs.gov) with 30 m resolution for slope calculations, watershed area delineation, and pour point analysis (Tables S1 and S2). Where the watershed exceeded 250,000 km^2, we utilized a DEM with 3-arc second resolution (Verdin, 2017). Analyses were completed using built-in algorithms within QGIS 3.4.6. Elevation for each sampling station was derived from Google© Earth, and precipitation and temperature data were obtained from WorldClim (Fick & Hijmans, 2017) (Table S1).

Bedload samples were collected directly from the active river channel axis and riverbanks, or from point bars where accessible, at stations with different lithologies and upstream and downstream of major confluences (Garzanti et al., 2013, 2015). We chose locations along the active channel that maximized sand content and avoided unstable or eroding riverbanks that may incorporate soil inputs. Basin-wide sampling stations were selected to maximize coverage across the Pantanal Basin, but the precise location was ultimately determined by physical accessibility and safety in mostly remote areas. We waded into the river to 0.5-1.0 m water column depth to collect the most recently deposited channel sediments or used a Van Veen sampler deployed from bridges. A total of 97 samples were collected across the six provenance regions (Figure 1). In the laboratory, each sample was air dried, sieved through a 2 mm sieve to remove grains larger than sand and 63 μm sieve to remove clays and silts, treated with 30% hydrogen peroxide, rinsed with deionized water, and air dried prior to thin section fabrication. Sand aliquots were sent to Wagner Petrographic (Lindon, Utah) for embedding in epoxy resin. Each slide was stained for calcite, plagioclase, and potassium feldspar. Five hundred (500) grains were counted in each sample following the Gazzi-Dickinson method (Table 1) (Ingersoll et al., 1985). Counts were completed on a Zeiss Photomicroscope equipped with a Swift point counter, with the spacing interval adjusted based on the average grain size in each thin section. Common grains were tabulated, and summary statistics were calculated for the full dataset. The

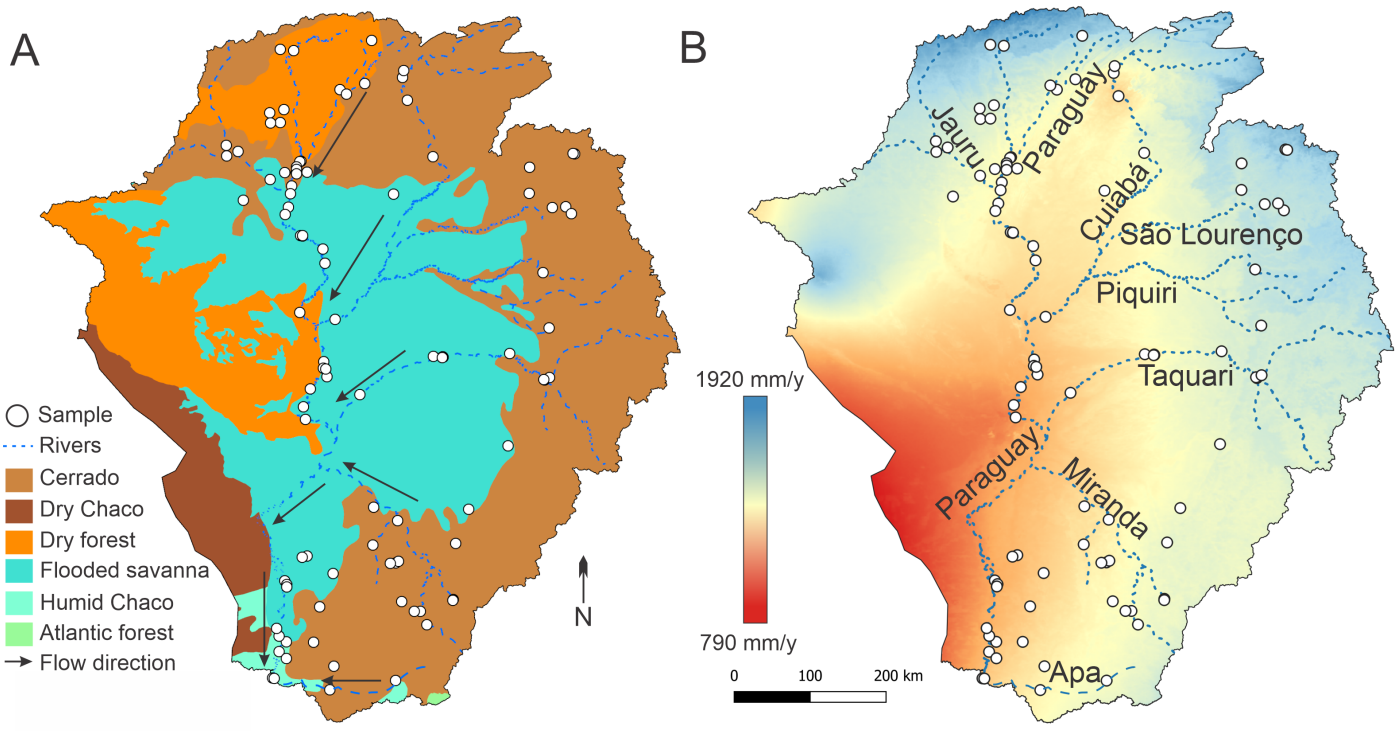

Figure 3 | (A) Vegetation ecoregions of the Pantanal Basin (Olson et al., 2001). The primary vegetation of the Pantanal consists of flooded savanna and cerrado (tropical savanna). (B) Mean annual precipitation (mm/y) from WorldClim database (Fick & Hijmans, 2017).

data were normalized and plotted on ternary diagrams using the provenance fields of Dickinson et al. (1983) and Dickinson (1985). The ratio Quartz/(Feldspar + Lithics) or Qt/(F+L) was calculated for each sample; larger values indicate greater intensity of weathering (Pettijohn, 1954).

Canonical correspondence analysis (CCA) was employed to examine the competing controls on sand composition. We considered the primary framework grain type determined in the point counts, total quartz (Qt), total feldspar (F), and total lithic clasts (L), along with the major hinterland lithologies and environmental variables. To facilitate this analysis, we grouped the hinterland lithologies into seven categories (Figure 2B). Sedimentary rocks were simplified and binned into siliciclastic or carbonate types. Metamorphic rocks were grouped into foliated or non-foliated lithotypes, and igneous rocks were divided into plutonic and volcanic lithotypes. We also considered the unconsolidated alluvium in the lowlands, which occupy a large proportion of the Pantanal Basin. Key environmental parameters were included in the assessment, such as in-channel distance to the confluence with the Paraguay River (a relative proxy of transport distance), elevation at the sampling station, and average precipitation, temperature, and slope at each pour point defined sub-watershed.

4. Results

The average basin-wide sample composition QtFL was 88\5\7, and the average Qt/(F+L) was 44 (Table S3) based on common framework grains (Figure 4). The pour point analyses across the Pantanal Basin (Figure 5) showed that siliciclastic sedimentary rocks and unconsolidated surficial deposits dominated most of the watersheds, particularly when the sampling station was situated in the lowlands or the plateau. The most lithologically diverse outcrops

Symbol	Definition	Symbol	Definition
Qm	Monocrystalline quartz	Qpq	Polycrystalline quartz
P	Plagioclase feldspar	K	Potassium feldspar
Cht	Chert	M	Phyllosilicates (biotite, muscovite, chlorite)
F	Total feldspar grains (P + K)	U	Unidentifiable grains
Ls	Sedimentary lithic grains	Qt	Total quartz grains (Qm + Qpq + Cht)
Lm	Metamorphic lithic grains	Qp	Polycrystalline quartz grains (Qpq + Cht)
Lv	Volcanic lithic grains	Lt	Total lithic grains (Qpq + Lm + Lv + Ls)
L	Ls + Lm + Lv	Acc	Accessory (clinopyroxene, hematite, chalcedony, hornblende)

Table 1 | Point counting parameters.

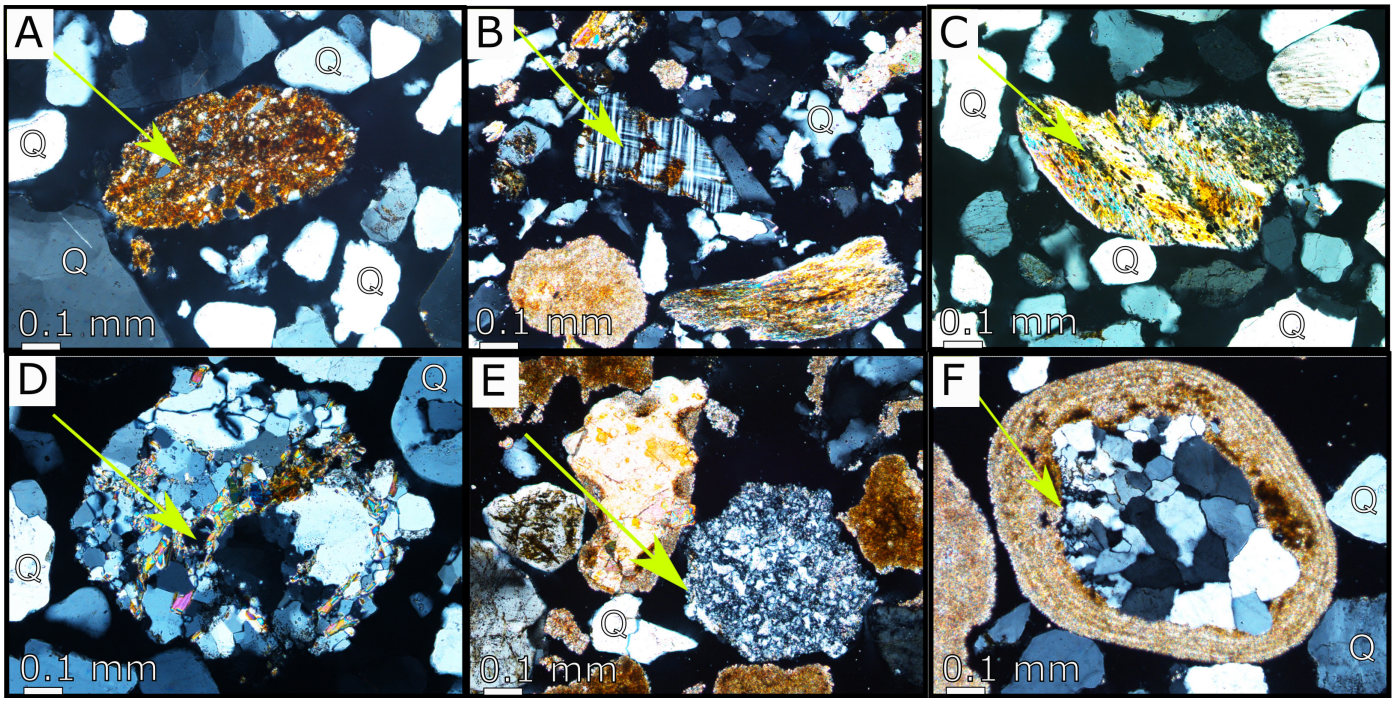

Figure 4 | Common framework grains identified with yellow arrows in thin sections from Pantanal Basin river sands. (A) detrital siltstone clast, (B) microcline, (C) lithic metamorphic grain, (D) polycrystalline quartz, (E) chert, and (F) ooid with polycrystalline quartz nucleus. Note the abundance of monocrystalline quartz grains (Q) in each panel and the calcite grains in (B) and (E).

were found in the watersheds draining the cratons and the Paraguay Belt.

4.1. Lowlands (Region A)

The lowland provenance domain is largely made up of low-elevation plains west of the plateau. The mean annual precipitation in the lowlands is 1430 mm, with an average annual temperature of 25°C. Lowland samples were derived from the largest watersheds (average 93,608 km^2) in the basin with large components of surficial alluvium and siliciclastic sedimentary lithotypes (A1-A39, Figure 5); only five of the 39 samples had >30% foliated metamorphic parent rocks in their sub-watersheds, all of which were derived from the smallest lowland watersheds.

The samples from the lowlands (Region A; n = 39) had the highest percentage of quartz grains for any of the Pantanal's provenance regions, with an average QtFL of 93\5\2 with a Qt/(F+L) range of 3 to >100 (average = 58) (Table S3). The lowland samples are most enriched in monocrystalline quartz, and all but three stations were quartzose (Figures 4, 6) (Dickinson, 1985). Lithic grains in lowland samples were predominantly sedimentary (Figure 4A). Considering the spatial variance of grain types in the lowlands, monocrystalline quartz grains were most common in proximity to the medial Paraguay River, near the geographic center of the Pantanal Basin (Figure 7).

4.2. Amazon Craton (Region B)

The Amazon craton provenance domain consists of hilly remnants of the Precambrian formations in the Jauru terrane in the northwest Pantanal Basin and the Sunsás province in eastern Bolivia. The mean annual precipitation is 1536 mm, with an average annual temperature of 26°C. Amazon craton samples were derived from relatively small watersheds (average 1,318 km^2) with extensive volcanic, plutonic, and foliated metamorphic lithotypes (B1-B9, Figure 5); only two of the nine samples had >50% siliciclastic sedimentary rocks in their sub-watersheds. The areal extent of the most common lithotypes was composed of 31% siliciclastic rocks, 22% plutonic igneous rocks, 18% volcanic igneous rocks, and 18% foliated metamorphic rocks averaged across the 9 Amazon craton sample watersheds (Table S2).

For samples from the Amazon craton provenance region (Region B; n = 9), the average QtFL was 92\5\3 with a Qt/(F+L) range of 6 to 69 (average = 22). Most Amazon craton samples were quartzose (Figure 6). Amazon craton samples belonged to three tributaries that originated from the northwestern Pantanal Basin. The spatial patterns of grain types showed that feldspar counts were ~5% and lithic grains were 2-3% except for one sampling station where the Qt/(F+L) was >30 (Figure 7). The feldspathic grains were further transported to the Paraguay River lowland samples immediately downstream of the confluences of the tributary rivers draining the Amazon craton.

4.3. Rio Apa Craton (Region C)

The Rio Apa craton is the southernmost exposure of the Amazonian craton and consists of outcrops covered by Quaternary sediments (Cordani et al., 2010; Faleiros et al., 2016). The mean annual precipitation is 1260 mm, with an average annual temperature of 25°C. Rio Apa craton samples were derived from an average watershed size

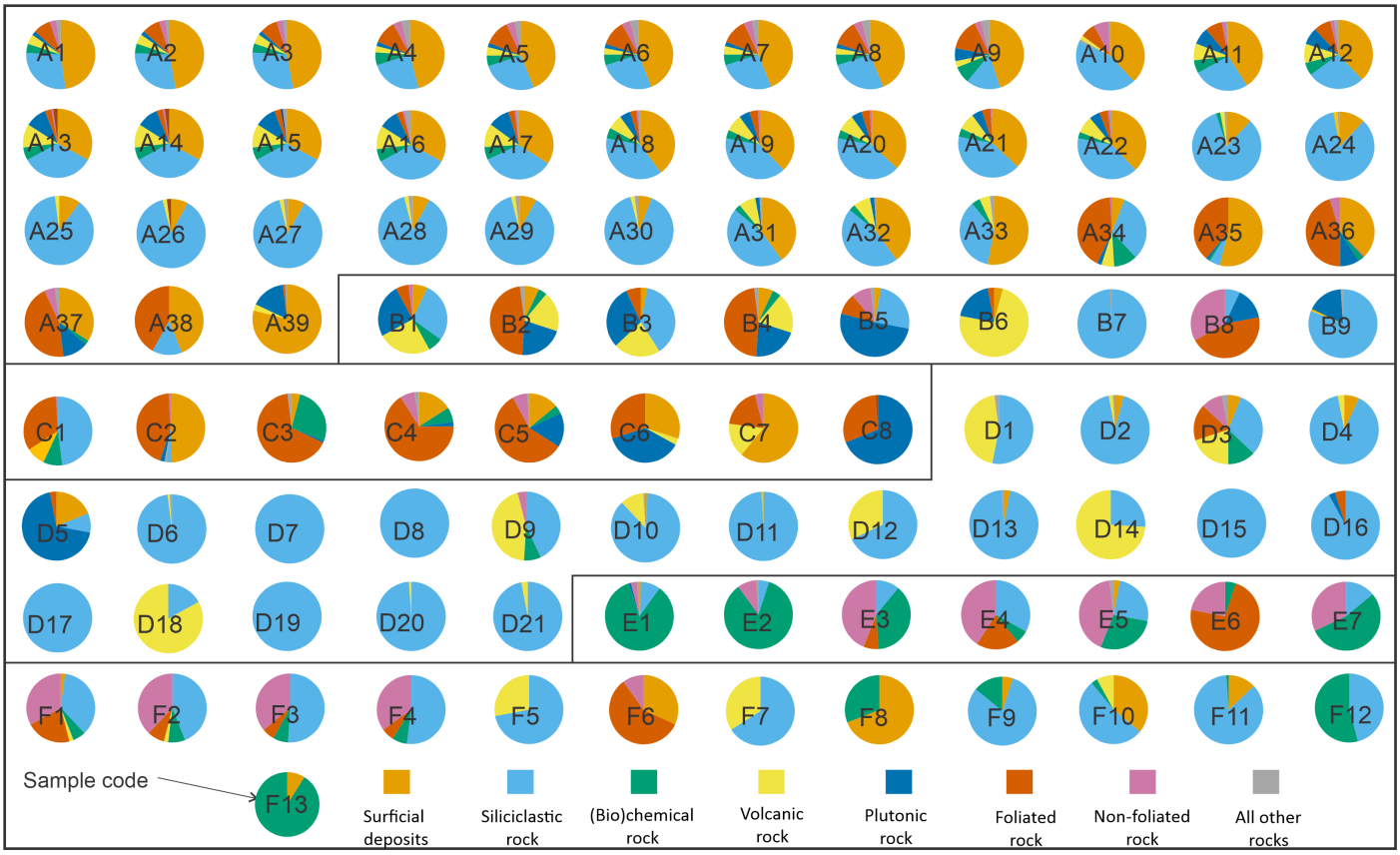

Figure 5 | Pie charts showing relative proportions of lithologies (see Figure 2B) in each sample sub-watershed resulting from pour point analysis. For each region, samples were organized by decreasing watershed size ordered left to right and top to bottom. Regions are A, Lowlands; B, Amazon craton; C, Rio Apa craton; D, Plateau; E, South Paraguay Belt; F, North Paraguay Belt.

of 2,774 km^2 draining foliated metamorphic lithologies and plutonic igneous rock. Only two of the eight samples contained >50% surficial sediments in the contributing area. The most common lithologies were 43% foliated metamorphic rocks, 22% surficial alluvial deposits, and 16% plutonic igneous rocks.

Samples from the Rio Apa craton provenance region (Region C; n = 8) had an average QtFL of 57\28\15, with a Qt/(F+L) range of 0 to 6 (average = 2). These samples are characterized as feldspatho-quartzose sands (Figure 4B). Rio Apa craton sands are the most enriched in potassium feldspar of any samples in the Pantanal Basin (Figure 6). The Qt/(F+L) decreased to <12 in the Paraguay River stations downstream of the confluence with tributary supply of feldspars sourced from the adjacent craton. Lithic grains are enriched to 20-89 grains/sample and Qt/(F+L) decreases to <20 in the downstream Paraguay River lowland samples.

4.4. Plateau (Region D)

The plateau river samples primarily drain Phanerozic-aged siliciclastic formations and volcanic igneous rocks (mainly dacite) and are characterized by deep, rapidly eroding gullies. The mean annual precipitation is 1516 mm, with an average annual temperature of 24°C. The plateau samples are derived from an average watershed size of 14,240 km^2. All but five samples have >50% siliciclastic lithologies in their watersheds. The areal extent of siliciclastic rocks was 76%, and volcanic igneous rocks averaged 15% across the plateau sample watersheds (Table S2).

Sand from the plateau provenance region (Region D; n = 21) show an average QtFL of 94\2\4 with a Qt/(F+L) range of 4 to >100 (average = 60). Like the lowland sands, the plateau sands were chiefly quartzose (Figure 6). With respect to spatial variance, a hinge in quartz enrichment was observed, with samples from the plateau south of the Taquari River being less quartzose than plateau samples north of the Taquari River. The southeast plateau samples had lower Qt/(F+L) and higher abundances of lithic and feldspar grains (Figure 7) (Barboza et al., 2018).

4.5. South and North Paraguay Belt (Regions E and F)

Both regions of the Paraguay Belt consist of a fold-thrust belt covered by Phanerozoic sediments. The mean annual precipitation is ~1314 mm in Region E and ~1493 mm in Region F, with an average annual temperature of 24°C and 25°C, respectively. Region E sample watersheds had an average watershed size of 384 km^2, and the Region F watershed average size was 6,816 km^2 draining Neoproterozoic metasediments and granites (Barboza et al., 2018).

The South Paraguay Belt samples Region E (n = 7) show an average QtFL of 52\3\45, with a Qt/(F+L) range of 0 to 21 (average = 4), and the North Paraguay Belt samples Region F (n = 13) were 96\0\4, with a Qt/(F+L) range of 9 to 160 (average = 41). The most commonly occurring lithologies

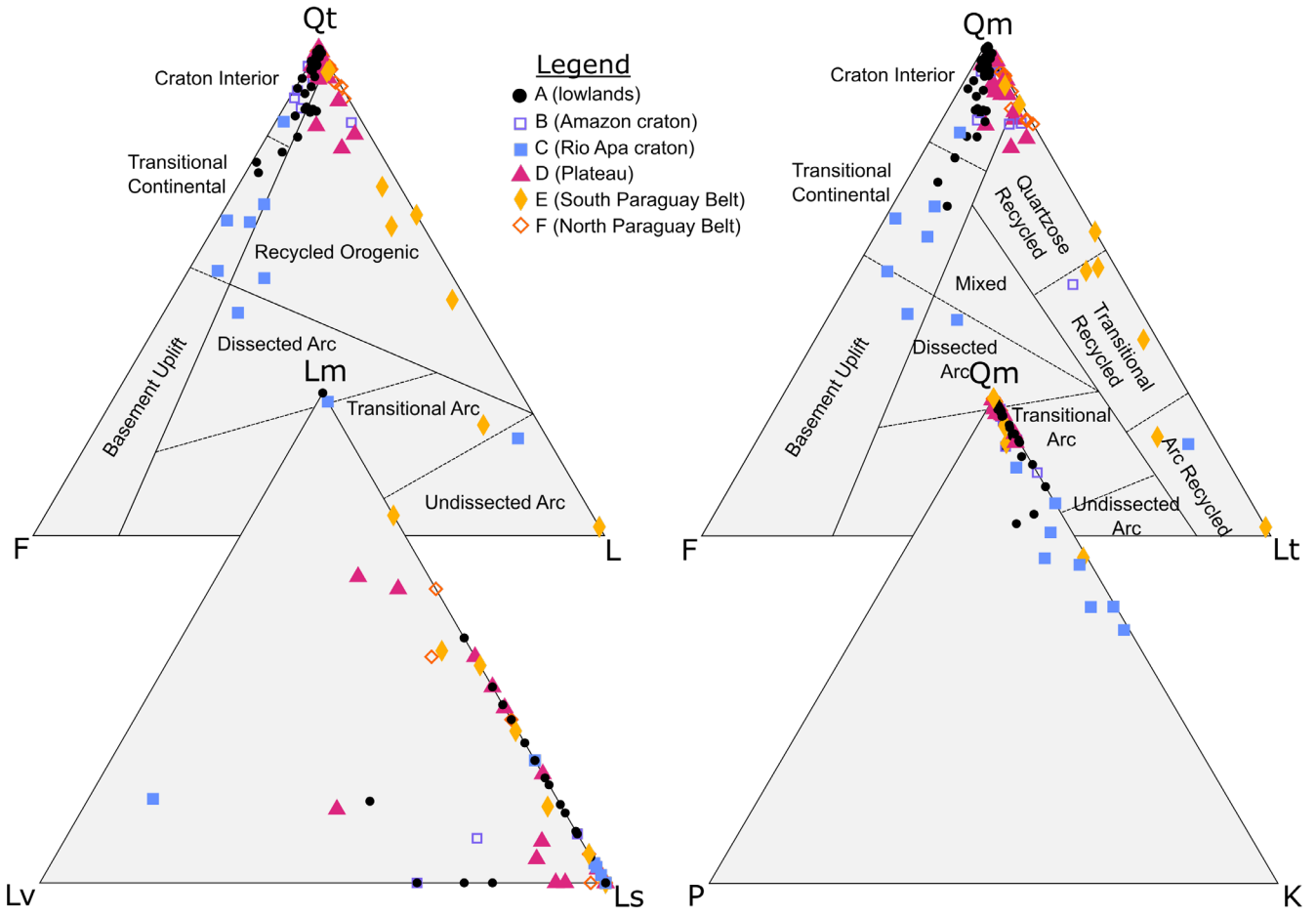

Figure 6 | Ternary plots of sand composition in the Pantanal Basin and its provenance regions (Dickinson, 1985). The vertices were Qt (sum of monocrystalline quartz, polycrystalline quartz, and chert), F (sum of plagioclase and potassium feldspar), and L (sum of lithic igneous, metamorphic, and sedimentary grains). Qm (monocrystalline quartz), F (plagioclase and potassium feldspar), and Lt (polycrystalline quartz and lithic igneous, metamorphic, and sedimentary grains). Lm (lithic metamorphic), Lv (lithic volcanic), and Ls (lithic sedimentary). Qm (monocrystalline quartz), P (plagioclase) and K (potassium feldspar).

in the South Paraguay Belt were carbonate sedimentary rocks (43%) and non-foliated metamorphic rocks (28%). The common lithologies in the North Paraguay Belt were siliciclastic rocks (45%) and biochemical sedimentary rocks (17%). The North Paraguay Belt sands had nearly double the quartz content of the South Paraguay Belt sands. South Paraguay Belt samples were characterized as litho-quartzose sand (Figure 4E). In contrast, North Paraguay Belt samples were depleted in feldspars (<2%) and lithic sediments (<4%).

4.6. Spatial distribution and statistical data

The spatial interpolation maps (Figure 7) provided a basin-wide visual representation of raw point counts. The areas with the highest total quartz counts were the medial Pantanal lowlands in the Paraguay River and the northeast Pantanal plateau. Only isolated samples in the southeast plateau, South Paraguay Belt, and the Rio Apa craton contained >478 quartz grains. The highest feldspar counts were found in the Rio Apa craton and in select lowland samples downstream of the Rio Apa craton. High lithic grain counts were concentrated in the South Paraguay Belt and in select samples of the Rio Apa craton. The Qt/(F+L) map showed that the highest values (>79) generally overlapped with the highest total quartz counts. The lowest Qt/(F+L) values (<13) overlapped with the highest feldspar and lithic grain counts in the South Paraguay Belt and the Rio Apa craton.

The canonical correspondence analysis (Figure 8) considered how a suite of environmental variables including precipitation, temperature, elevation, slope, and distance from the Paraguay River and surficial extent of lithotypes influence riverine sand composition. Rainfall, temperature, average slope, and metamorphic and sedimentary lithologies were important along component 1. The average watershed slope and metamorphic lithologies exerted the strongest control on samples in the South Paraguay Belt and the Rio Apa craton. These environmental and lithological characteristics translated into greater feldspar counts in Rio Apa sands and sedimentary lithic grains in South Paraguay Belt sands. Most of the closely grouped samples from the lowlands, Amazon craton, plateau, and North Paraguay Belt regions loaded negatively on component 1, where the mean annual precipitation was a strong predictor for sand composition. Component 2 was most influenced by sampling station elevation, proportion of

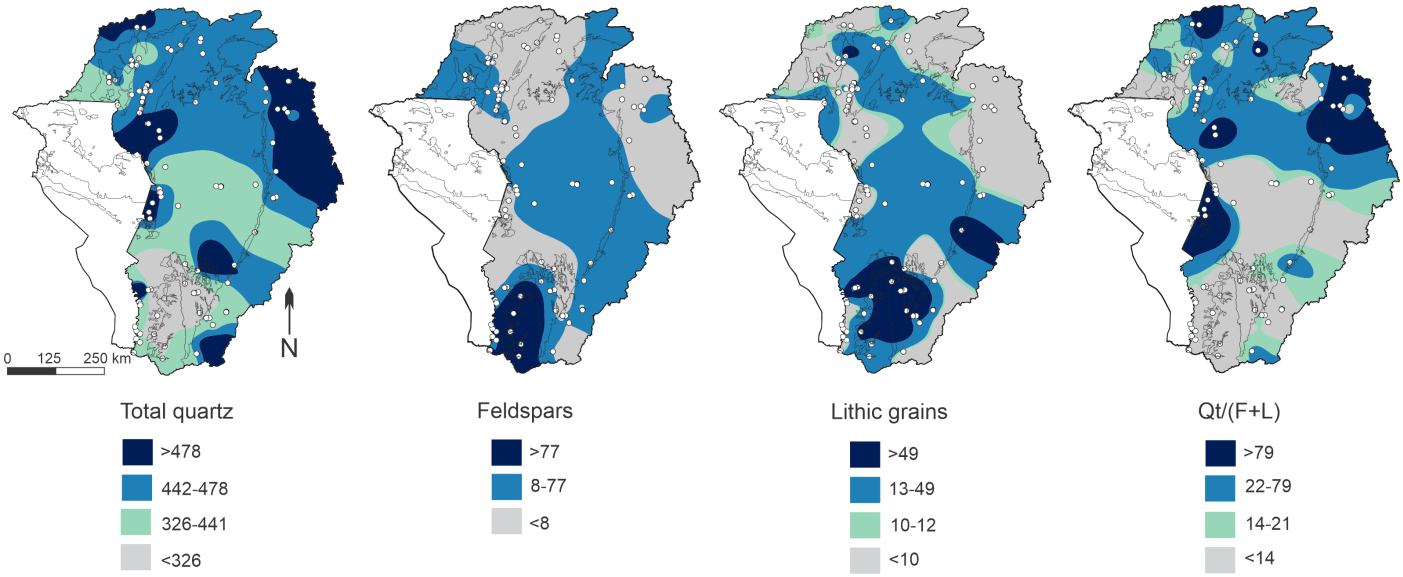

Figure 7 | Spatial interpolation maps of the Upper Paraguay River Basin showing raw point counts for Qt (sum of monocrystalline quartz, polycrystalline quartz, and chert), F (sum of plagioclase and potassium feldspar), and L (sum of lithic igneous, metamorphic, and sedimentary grains) and Qt/(F+L). Blank areas have no data. Maps are overlaid with outlines of provenance areas shown in Figure 1B.

sedimentary parent rocks, and distance from the Paraguay River.

5. Discussion

5.1. The modern Pantanal back-bulge in the Andean retroarc context

Modern sediments in the Pantanal Basin are assumed to originate entirely from the interior craton. Several westward directed fluvial fans occupy the Pantanal Basin, with their apex defined by the transition from plateau to lowland provenance domains. The largest examples of these are the Paraguay, Cuiabá, São Lourenço, and Taquari fans with smaller examples in the inter-megafan area (e.g., Weissmann et al., 2015). The smaller fluvial fans such as the Miranda River fan are adjacent to interfan plains (Merino & Assine, 2020). These rivers all discharge into the Paraguay River, which serves as the trunk river or axial fluvial system. The dominance of sand in all of these areas suggests low accommodation compared to sediment supply (Weissmann et al., 2015). As a result of this basin configuration, practically no Andean syn-orogenic sediment is transported by rivers into the Pantanal Basin, which is instead filled with non-orogenic cratonic debris. Contributions of wind-blown sand to the Pantanal are unknown, but given prevailing wind directions at the latitude of the basin, the effects of eolian deposition are presumed to be minimal.

The Pantanal Basin sediments were considered in the context of the modern regional Andean river sands studied closer to the extant fold-and-thrust belt (Decelles & Hertel, 1989; Savage & Potter, 1991; Vezzoli et al., 2013; McGlue et al., 2016; Garzanti et al., 2021a, b). The sands downstream of four of the six provenance regions were highly quartzose (>90 % quartz) (Figure 9), consistent with a cratonic interior source (Dickinson et al., 1983; Dickinson, 1985). This assemblage contrasts with other areas of the Andean back-bulge that are connected to the thrust front by rivers that traverse the forebulge crest, such as the Pilcomayo and Bermejo Rivers, which discharge into the Paraguay River from the west (Cohen et al., 2015; McGlue et al., 2016). Both the Pilcomayo and Bermejo Rivers have similar quartzose compositions at their confluence with the Paraguay River, but in those cases, sediments were derived from the recycling of Subandean Belt siliciclastic rocks. The key exceptions to high quartz content in the Pantanal Basin were the sands from the Rio Apa craton and the South Paraguay Belt, reflecting compositionally distinct Precambrian sources of sediment generation. These relatively diverse sand compositions can be ascribed to tributaries draining crystalline basement. The modern Pantanal Basin fluvial sands provide key data to improve our understanding of back-bulge sedimentary processes, particularly as sand petrology datasets are used to train predictive machine learning models (Johnson et al., 2022).

5.2. Lithology as a primary control on sand generation

Sands from the Pantanal Basin are quartzose, which is consistent with the source lithologies of siliciclastic sedimentary rocks and alluvium occupying ~80% of the basin's surface area. The large fluvial megafans of the Paraguay, Taquari, and Cuiabá fans are responsible for most of the alluvial cover and drain fine- to medium-grained quartz arenites of fluvial or eolian origins in the plateau region (Fantin-Cruz et al., 2020). The Bauru, Botucatu, and Aquidauana formations were the most likely origins of these sediments based on their composition (Wu & Caetano-Chang, 1992; Schiavo et al., 2010; Fernandes & Magalhães Ribeiro, 2015). Commonly sub-rounded and rounded grains in the Paraguay River samples suggested that a proportion of the sands originated from the Botucatu

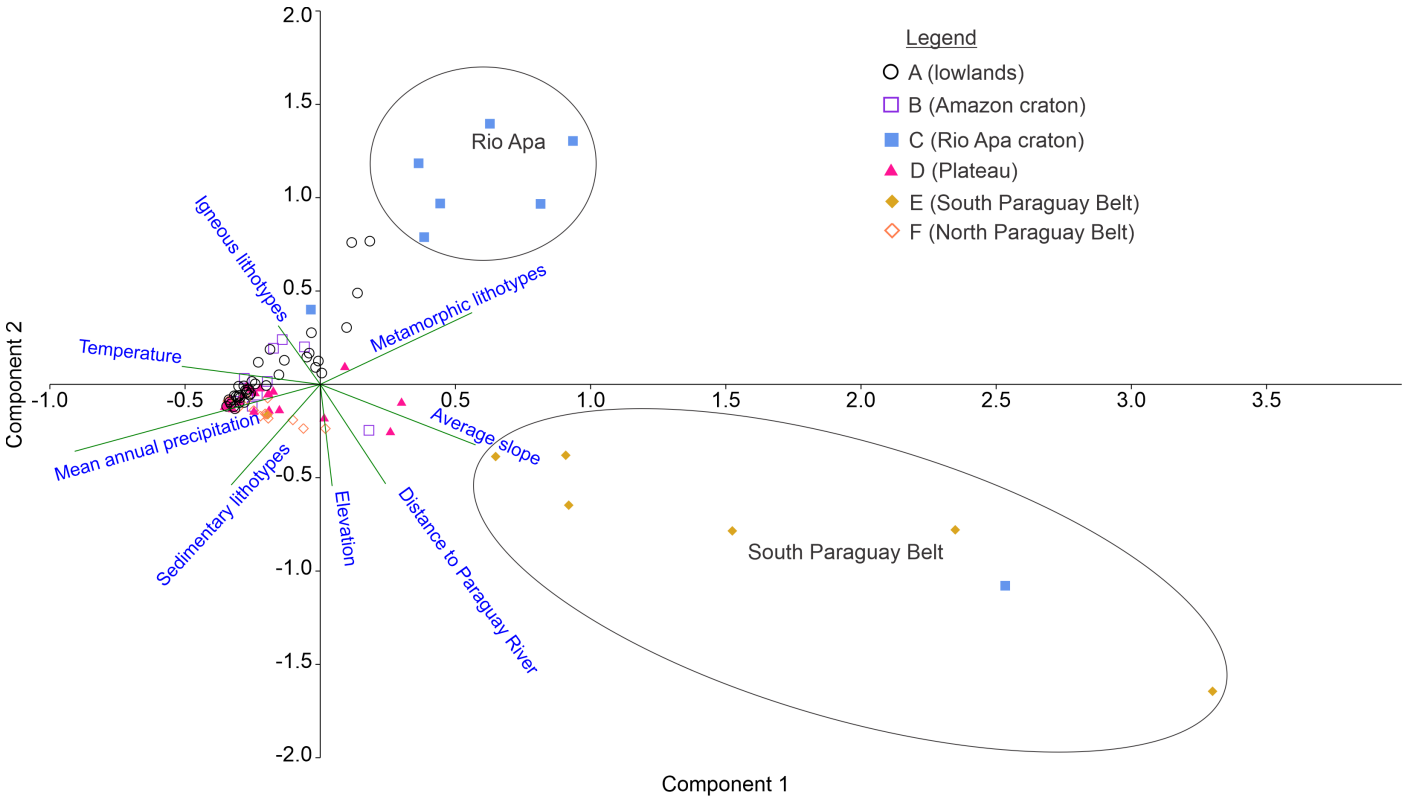

Figure 8 | Canonical correspondence analysis (CCA) plot showing how distance to the Paraguay River, temperature, average slope, elevation, igneous rock, metamorphic rock, and sedimentary rock/alluvium affect Qt, F, L. The compositional biplot shows sampling stations (points) and variables (green rays). Longer rays are proportional to the variance of the corresponding element in the data set.

Formation eolian sands (Bertolini et al., 2021). Taking the Bauru Formation as a representative contributing unit, soils developing over these lithologies are quartz-rich ferralsols influenced by intense chemical weathering associated with prolonged exposure to high temperature and precipitation (Balbino et al., 2002). Given these extensive weathering conditions and source areas composed of arenites, multiple phases of quartz recycling are very likely to have occurred in the sediment-generating hinterland.

For most rivers, quartz sand counts generally increased towards the lowland region, as the distance to the Paraguay River confluence decreased. Some exceptions to this trend are present, however. Litho-feldspatho-quartzose sand originated from Rio Apa foliated metamorphic rocks in the Alto Tererê Group and the Amoguijá Group (Figure 9) (RadamBrasil, 1982). Litho-quartzose sand originated from the South Paraguay Belt biochemical sedimentary rocks and non-foliated metamorphic rocks in the Corumbá Group and the Cuiabá Group, respectively (Figure 9) (RadamBrasil, 1982). The size of the watershed may also play an important role, because only sands from small watersheds (on average <2000 km^2) preserved lithic grains. By analogy, changes in quartz percentage were observed in the equatorial Kagera River (East Africa) due to dilution (e.g., Garzanti et al., 2013). Dilution with quartz may increase with watershed size in the Pantanal Basin, and therefore influence river sand composition.

Within the Paraguay River, sands become increasingly fine and quartzose traveling from north to south. However, the composition of Paraguay River sand was modified as the river flowed adjacent to the Rio Apa craton south of the Miranda River confluence (Figure 7). The Paraguay River samples near the Rio Apa craton have greater feldspar counts by virtue of their proximity to the foliated metamorphic rocks and plutonic igneous rocks in the hinterland outcrops. Additional samples from the Paraguay River in Paraguayan territory may help clarify the spatial influence of the Rio Apa craton on sand composition beyond the initial confluence with the Paraguay River. Studying the Paraguay River terraces may also help to constrain the history of sediment generation and export (Jonell et al., 2017).

5.3. Chemical weathering as a secondary control on sand composition

Differences in hydroclimate may constitute a feedback mechanism on sediment generation processes and help to explain the higher counts of lithic sedimentary grains and feldspars in the southern half of the Pantanal Basin. Chemical weathering in the Pantanal Basin is determined by seasonally and spatially variable precipitation and temperature (Figure 3B). The mean annual precipitation appears to be a secondary influence on the modern river sand composition in the Pantanal Basin based on the multivariate statistics (Figure 8). The southern Pantanal, where the Rio Apa and South Paraguay Belt provenance regions are situated, has a shorter dry season of 1 to 3 months, and reduced mean annual precipitation, resulting in less efficient weathering and transport of sediments. We

inferred that >1300 mm/y of precipitation coupled with a dry season of 4-5 months in the plateau provenance region led to more effective weathering and flushing of quartz-rich sand (Latrubesse et al., 2012). The export of quartz grains from the siliciclastic lithotypes is therefore interpreted to be an important control on lowland, Amazon craton and plateau sample composition, reflecting polyphase recycling and elevated tropical weathering rates.

One area of the lowlands that showed a divergence in the quartzose sand was the medial Taquari River megafan, which contained slightly higher abundances of fine-grained feldspar (up to 17% of the composition). We interpret that feldspars are concentrated in the finest sand size fraction, because hydrolysis exploits weaknesses in bond strength along cleavage planes. This reaction rapidly reduces feldspar grain size, especially for plagioclase grains (Suttner & Dutta, 1986; Islam et al., 2002).

The extent of soil development can produce sand compositions that are skewed towards higher quartz content from the hinterland regions. The steeper areas in the Serra da Bodoquena and Província Serrana have comparatively thin, poorly weathered lithosols, which facilitates an increased volume of sediment exported to the lowlands (Figure 1C) (Brosens et al., 2020). Fluvial sediments downstream of these steeper fold-thrust regions should contain more feldspar and lithic grains, which was observed for Rio Apa and South Paraguay Belt samples (Figure 7). The North Paraguay Belt samples downstream of the Província Serrana did not record as many feldspar and lithic grains, due to higher rainfall. Feldspar and lithic grains are rapidly weathered in the soils where the Pantanal's tropical climate prolongs chemical weathering (Berner & Holdren, 1979).

For the plateau region, the most strongly weathered soils (i.e., ferralsols) developed on the gently sloping areas of the plateau are known to generate more quartz-rich sediments (Deckers et al., 2003; Strey et al., 2016; Terra et al., 2018). The arenosols are poorly developed soils with high sand content and in fluvial deposits (Grossman, 1983). Where sandy soils form, the removal of feldspars likely occurs during periods of prolonged subaerial exposure and leaching. In contrast, the planosols are characterized by hydromorphized conditions and develop in the lowland regions (Benedetti et al., 2011). Both arenosols and ferralsols favor the generation of quartz-rich sediments, especially when combined with high temperature and precipitation encountered in the north and central areas of the basin (Sileshi et al., 2022). We observed this effect in the São Lourenço and Piquiri Rivers, where total quartz exceeds 93%.

Calcite grains observed in a few samples of the South Paraguay Belt rivers suggest two simultaneous processes that are unique to specific localities in the Pantanal Basin. First, the breakdown of carbonate lithologies generates carbonate rock fragments. The carbonate formations consist of Xaraiés and Pantanal de Miranda limestones and the Serra da Bodoquena tufa deposits and other biogenic carbonates (Boggiani et al., 1995; Ribeiro et al., 2001; Oste et al., 2021). The sands of the Salobra River in the South Paraguay Belt region contain many (~66%) weathered carbonate grains, interpreted to be the result of weathering of the original limestone outcrops comprising >80% of the watershed surface area (Figure 4B, E, F). This finding was consistent with the underrepresentation of carbonate grains relative to their areal extent (Garzanti et al., 2021c). Second, the reduced annual rainfall and the carbonate formations help sustain high calcium concentrations in the surface waters, leading to penecontemporaneous calcite precipitation (Arribas & Arribas, 2007). Bicarbonate waters flow through these areas, and the occurrence of limestone deposits overlying Holocene sands likely facilitated the bicarbonate solution to precipitate ooids (Ribeiro et al., 2001; Silva et al., 2017). Freshwater ooids have been documented to form with microbial activity where shallow ponded water occurs (Davaud & Girardclos, 2001; Pacton et al., 2012). Although rarely reported, fluvial ooids have formed in areas that receive calcium carbonate-rich springs (Geno & Chafetz, 1982). The Formoso River in the South Paraguay Belt is filled with calcareous bioclastic sediment, counted as carbonate lithic grains (Oste et al., 2021). The E1, E3, E5, and E7 sampling stations contained >16% carbonate lithic sedimentary grains and 2% up to 10% feldspars. Hence, very localized processes influence sand compositions but become rapidly diluted by quartzose sands downstream of the confluence with the Miranda River.

5.4. Other landscape factors and implications

Vegetation composition can play an important role in sediment retention or export. The Apa craton, plateau, and South and North Paraguay Belt regions were historically dominated by savannas, with small areas of forest and grassland (Rodrigues et al., 2022). Their density and root structures help to retain sediments in the plateau regions and reduce sediment export to the lowlands both in the *cerrado* and the dry forest ecotones (Figure 3A). However, as humidity increased in the late Quaternary, the highly weathered ferralsols and arenosols would have been susceptible to eroding into the lowlands. More recently, land-use transitions have converted large swathes of the plateau into cropland and pasture (Godoy et al., 2002; Rodrigues et al., 2022). In order to determine the timing and volume of sediment export into the lowlands, the acquisition and dating of sediment cores from paleochannels is required (e.g., Pupim et al., 2017).

Two possibilities may explain the increased concentration of feldspar grains in the medial Taquari River megafan: reworking of buried floodplain sediments at the channel avulsions or unusual hydrodynamic sorting. Here, we focus on the reworking process. The Caronal avulsion is actively shifting the downstream half of the river to a new channel (Buehler et al., 2011; Louzada et al., 2020, 2021). The A26 and A27 sampling stations are located at the Caronal

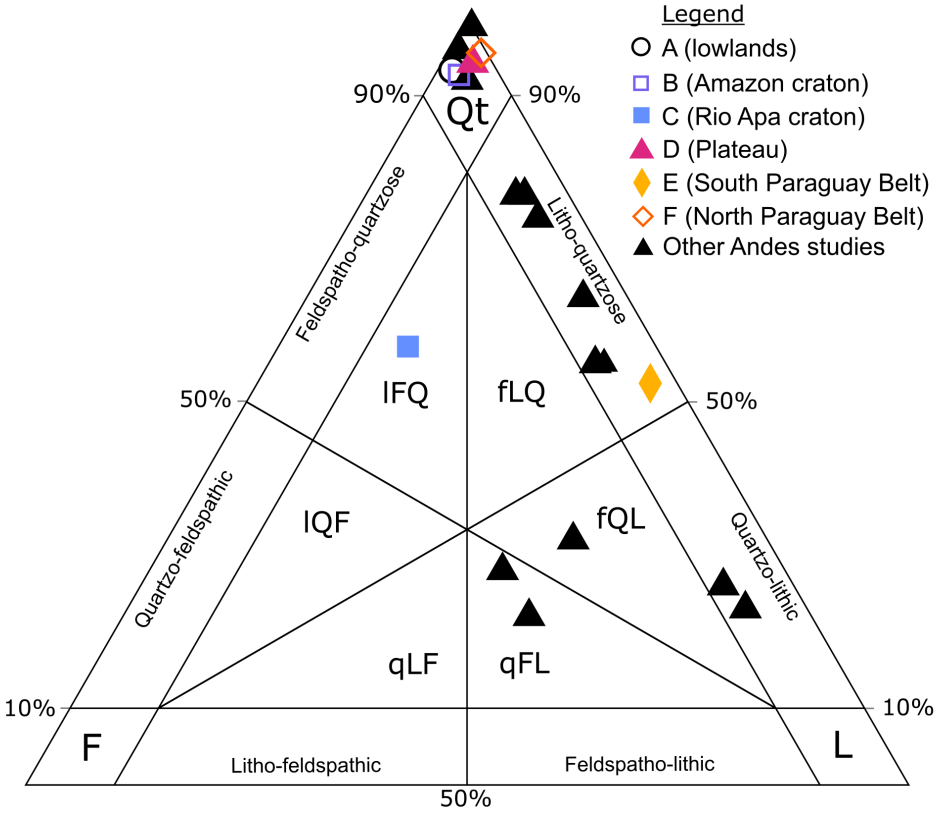

Figure 9 | Qt (sum of monocrystalline quartz, polycrystalline quartz, and chert), F (sum of plagioclase and potassium feldspar), and L (sum of lithic igneous, metamorphic, and sedimentary grains) ternary plot containing the average value for each of the six provenance regions as well as average QtFL values represented as black triangles reported from studies that used the Gazzi-Dickinson point counting protocol (Decelles & Hertel, 1989; Savage & Potter, 1991; Vezzoli et al., 2013; McGlue et al., 2016; Garzanti et al., 2021a). Abbreviations are defined lFQ = litho-feldspatho-quartzose, lQF = litho-quartzo-feldspathic, qLF = quartzo-litho-feldspathic, qFL = quartzo-feldspatho-lithic, fQL = feldspatho-quartzo-lithic, fLQ = feldspatho-litho-quartzose (Garzanti, 2019).

avulsion node where the Taquari River is constructing a new lobe and illustrate that very fine feldspars are rapidly redirected to the newly constructed channel, more than doubling the feldspar grains counted in the abandoned channel stations. The feldspar grains in the Cuiabá River (sample A10) comparable to those in the Taquari River might be explained by the sampling station's proximity to abandoned distal channel lobes that may supply reworked feldspathic grains. Because the downstream concentration of feldspars was observed primarily in or near these fluvial fans, we propose that channel avulsions and the subsequent incision of a new channel into the floodplain rework feldspars. These feldspar grains may have been deposited during the drier conditions of the early Holocene (Novello et al., 2017; McGlue et al., 2017).

The composition of sand along rivers depends in part on the grain size but why this occurs remains debated (Garzanti et al., 2009; Miller et al., 2014). It is useful to consider how grain size may influence the sand composition (63-2000 μm). The Taquari River contained moderate amounts of potassium feldspar grains and chert, but in the medial Taquari megafan, the raw count of feldspar grains increased due to a grain size effect where feldspathic grains are commonly reduced to very fine sand size (Odom, 1975; Garzanti et al., 2008). Much of the surface sediment in the Pantanal is reworked by fluvial channel processes (Assine et al., 2015; Pupim et al., 2017). Hydraulic sorting effects have been shown to change grain size distribution and can be identified by a few characteristics (Kroonenberg, 1992; Barshep & Worden, 2023). We propose that selective entrainment of finer, less dense grains such as feldspars compared with quartz grains is a common process in the Pantanal (Komar, 1987). Although sorting and grain size were not explicitly measured, Taquari River sands became finer from the plateau towards the Caronal avulsion. When the Taquari distributary channels discharge into the Paraguay River, the high Qt/(F+L) values where quartz content is >90% and increasingly fine sands suggest that grain size and composition are linked.

Slope is another important factor related to the potential for sediment generation, particularly along the hinterland plateau regions. The siliciclastic formations in the plateau region are friable and weakly consolidated, which eases and hastens the development of dendritic drainage and erosion. The extensively weathered arenosols and ferralsols forming on these lithologies can be a critical source of fine grains observed in the lowlands. In contrast, the steeper gradient of the Paraguay Belt precludes deeper soil profiles and instead facilitates the export of comparatively poorly weathered feldspathic and lithic grains. Low gradient in the floodplains can help increase the possibility that the grains are diluted or incorporated into soil-forming processes (Hatzenbühler et al., 2022).

6. Conclusions

We evaluated lithologic and hydroclimate controls on sand production in the modern rivers of the Pantanal Basin, the largest extant example of a back-bulge basin. Petrographic data were combined with remotely sensed datasets to determine the factor(s) that influence modern sand composition. River sands were predominantly quartzose in the Pantanal and consisted of non-orogenic debris. The other two endmembers were feldspatho-quartzose sand and litho-quartzose sand from the Rio Apa craton and the South Paraguay Belt, respectively. Intensive weathering, consistent with the seasonally wet tropical environment, was evident from the condition of the minerals in thin section, as lithic fragments were only present in smaller, steeper watersheds draining the Rio Apa and the South Paraguay Belt. The presence of carbonate lithic sands was spatially limited to small, upland regions related with bicarbonate waters.

We found that parent rock lithology was the primary control on modern sand composition in the Pantanal Basin, with secondary effects from spatial climate variability. The average slope helped to explain the presence of lithic grains; areas of higher average watershed slope and therefore more rapid transfer into the sediment routing system usually had more lithic grains. Areas of lower slope and therefore increased storage capacity in the floodplain favored more quartz grains. Lithic compositional signals were rapidly lost downstream in areas with steep topography and felsic volcanic rocks. Chemical weathering driven by variable precipitation and seasonality acted as a secondary control on sand composition in the Pantanal Basin. This effect was most evident in the rapid loss of less durable feldspars and lithics as dilution from tributary supply increased downstream. Most of these lithic grains were present when the sampling station was in an area with adjacent geologic outcrops to supply freshly weathered grains. Critically, the increased feldspar counts in the fine fraction of the Taquari River megafan were interpreted to occur from the reworking of floodplain deposits as avulsions incised new channels, tapping into older, more feldspar-rich deposits that may have accumulated under drier conditions of the early Holocene.

The sands of the Pantanal Basin demonstrate the usefulness of the Qt/(F+L) ratio as an overall indicator for the influence of different provenance regions. Regions south of the Taquari River and along the Taquari River have Qt/(F+L) <30, contrasting with areas that have Qt/(F+L) >120 north of the Taquari River apart from the Amazon craton. Refining sand genesis models of back-bulge basin environments in the sedimentary record will require a cautious assessment of paleoclimate and hinterland geology.

Acknowledgments

This material is based upon work supported by the National Science Foundation Graduate Research Fellowship Program under Grant No. 1839289. This work was partially supported by a Southern Regional Education Board Doctoral Scholars Program Dissertation Award, two Ferm Fund awards from the Department of Earth and Environmental Sciences at the University of Kentucky, and an NSF/GSA Graduate Student Geoscience Grant #12743-20, which was funded by NSF Award #1949901 to E. Lo. The study received support from the *Conselho Nacional de Desenvolvimento Científico e Tecnológico* (CNPq - Processes: 314986/2020-0 and 431253/2018-8) and a *Bolsa PQ* to A. Silva (Process: 314986/2020-0). The *Fundação de Apoio ao Desenvolvimento do Ensino, Ciência e Tecnologia do Estado de Mato Grosso do Sul* (FUNDECT - Processes: TO 267/2022 and 063/2017) financed fieldwork and research development. This study was supported by the *Fundação Universidade Federal de Mato Grosso do Sul* – UFMS/MEC – Brazil. P. Idstein graciously provided access to a Swift point counter and petrographic microscope. Thanks to P. Mendez of the *Gobierno Autónomo Departamental de Santa Cruz* for sharing geologic GIS datasets. We are indebted to L. Matchua Souza of the Kadiwéu leadership for access to two sampling stations located in the Kadiwéu indigenous territory. We thank reviewers E. Garzanti and I. Kane for their valuable comments and advice, which have greatly improved this manuscript.

Authors contribution

Conceptualization: E.L.L., M.M.M., and A.S. Logistics and fieldwork: G.G.R., A.S., E.L.L., S.K., and R.O.L. Lab analyses: E.L.L. Writing and figure development: E.L.L., M.M.M., and G.G.R. All authors have read and agreed to the published version of the manuscript.

Data availability

All of our relevant datasets are included in supplementary materials.

Conflict of interest

The authors declare that they have no known competing financial interests or personal relationships that could have appeared to influence the work reported in this paper.

References

Alvarenga, C. J. S., Boggiani, P. C., Babinski, M., Dardenne, M. A., Figueiredo, M. F., Dantas, E. L., Uhlein, A., Santos, R. V., Sial, A. N., & Trompette, R. (2011). Chapter 45 Glacially influenced sedimentation of the Puga Formation, Cuiabá Group and Jacadigo Group, and associated carbonates of the Araras and Corumbá groups, Paraguay Belt, Brazil. Geological Society, London, Memoirs, 36(1), 487–497. https://doi.org/10.1144/M36.45

Alvares, C. A., Stape, J. L., Sentelhas, P. C., de Moraes Gonçalves, J. L., & Sparovek, G. (2013). Köppen's climate classification map for Brazil. Meteorologische Zeitschrift, 22(6), 711–728. https://doi.org/10.1127/0941-2948/2013/0507

Arribas, M. E., & Arribas, J. (2007). Interpreting carbonate particles in modern continental sands: An example from fluvial sands (Iberian Range, Spain). In J. Arribas, M. J. Johnsson, & S. Critelli (Eds.), Sedimentary Provenance and Petrogenesis: Perspectives from Petrography and Geochemistry (Vol. 420, p. 167-179). Geological Society of America. https://doi.org/10.1130/2006.2420(11)

Assine, M. L. (2005). River avulsions on the Taquari megafan, Pantanal wetland, Brazil. Geomorphology, 70(3), 357–371. https://doi.org/10.1016/j.geomorph.2005.02.013

Assine, M. L., Merino, E. R., Pupim, F. do N., Macedo, H. de A., & Santos, M. G. M. dos. (2015). The Quaternary alluvial systems tract of the Pantanal Basin, Brazil. Brazilian Journal of Geology, 45, 475–489. https://doi.org/10.1590/2317-4889201520150014

Assine, M. L., Merino, E. R., Pupim, F. do N., Warren, L. V., Guerreiro, R. L., & McGlue, M. M. (2016). Geology and geomorphology of the Pantanal Basin. In I. Bergier & M. L. Assine (Eds.), Dynamics of the Pantanal Wetland in South America (pp. 23–50). Springer International Publishing. https://doi.org/10.1007/698_2015_349

Assine, M. L., & Silva, A. (2009). Contrasting fluvial styles of the Paraguay River in the northwestern border of the Pantanal wetland, Brazil. Geomorphology, 113(3), 189–199. https://doi.org/10.1016/j.geomorph.2009.03.012

Balbino, L. C., Bruand, A., Brossard, M., Grimaldi, M., Hajnos, M., & Guimarães, M. F. (2002). Changes in porosity and microaggregation in clayey Ferralsols of the Brazilian Cerrado on clearing for pasture. European Journal of Soil Science, 53(2), 219–230. https://doi.org/10.1046/j.1365-2389.2002.00446.x

Barboza, E., Santos, A., Fernandes, C., & Geraldes, M. (2018). Paraguay Belt lithostratigraphic and tectonic characterization: implications in the evolution of the orogen (Mato Grosso-Brazil). Journal of Sedimentary Environments, 3, 54–73. https://doi.org/10.12957/jse.2018.34219

Barshep, D. V., & Worden, R. H. (2023). Hinterland environments of the Late Jurassic northern Weald Basin, England. Geological Journal, 58(7), 2555-2577. https://doi.org/10.1002/gj.4720

Benedetti, M. M., Curi, N., Sparovek, G., Carvalho Filho, A. de, & Silva, S. H. G. (2011). Updated Brazilian's georeferenced soil database – an improvement for international scientific information exchanging. In Principles, Application, and Assessment in Soil Science (p. 408). https://doi.org/10.5772/29627

Berner, R. A., & Holdren, G. R. (1979). Mechanism of feldspar weathering—II. Observations of feldspars from soils. Geochimica et Cosmochimica Acta, 43(8), 1173–1186. https://doi.org/10.1016/0016-7037(79)90110-8

Bertolini, G., Marques, J. C., Hartley, A. J., Basei, M. A. S., Frantz, J. C., & Santos, P. R. (2021). Determining sediment provenance history in a Gondwanan erg: Botucatu formation, Northern Paraná Basin, Brazil. Sedimentary Geology, 417, 105883. https://doi.org/10.1016/j.sedgeo.2021.105883

Boggiani, P. C., Coimbra, A. M., & Coutinho, J. M. V. (1995). Quaternary limestones of the Pantanal area, Brazil. Anais Da Academia Brasileira de Ciências, 67(3), 343–349.

Braga, L. G., Pierosan, R., & Geraldes, M. C. (2019). Paleoproterozoic (2.0 Ga) volcano-plutonism in the southeastern region of the Amazon Craton: Petrological aspects and geotectonic implications. Geological Journal, 55(6), 4352–4374. https://doi.org/10.1002/gj.3686

Bravo, J. M., Allasia, D., Paz, A. R., Collischonn, W., & Tucci, C. E. M. (2012). Coupled hydrologic-hydraulic modeling of the Upper Paraguay River Basin. Journal of Hydrologic Engineering, 17(5), 635–646. https://doi.org/10.1061/(ASCE)HE.1943-5584.0000494

Brosens, L., Campforts, B., Robinet, J., Vanacker, V., Opfergelt, S., Ameijeiras-Mariño, Y., Minella, J. P. G., & Govers, G. (2020). Slope gradient controls soil thickness and chemical weathering in subtropical Brazil: Understanding rates and timescales of regional soilscape evolution through a combination of field data and modeling. Journal of Geophysical Research: Earth Surface, 125(6), e2019JF005321. https://doi.org/10.1029/2019JF005321

Buehler, H. A., Weissmann, G. S., Scuderi, L. A., & Hartley, A. J. (2011). Spatial and temporal evolution of an avulsion on the Taquari River distributive fluvial system from satellite image analysis. Journal of Sedimentary Research, 81(8), 630–640. https://doi.org/10.2110/jsr.2011.040

Capaldi, T. N., George, S. W. M., Hirtz, J. A., Horton, B. K., & Stockli, D. F. (2019). Fluvial and eolian sediment mixing during changing climate conditions recorded in Holocene Andean foreland deposits from Argentina (31–33°S). Frontiers in Earth Science, 7, 298. https://doi.org/10.3389/feart.2019.00298

Carrapa, B., Trimble, J. D., & Stockli, D. F. (2011). Patterns and timing of exhumation and deformation in the Eastern Cordillera of NW Argentina revealed by (U-Th)/He thermochronology. Tectonics, 30(3). https://doi.org/10.1029/2010TC002707

Cedraz, V., Julià, J., & Assumpção, M. (2020). Joint inversion of receiver functions and surface-wave dispersion in the Pantanal wetlands: Implications for basin formation. Journal of Geophysical Research: Solid Earth, 125(2), e2019JB018337. https://doi.org/10.1029/2019JB018337

Chase, C. G., Sussman, A. J., & Coblentz, D. D. (2009). Curved Andes: Geoid, forebulge, and flexure. Lithosphere, 1(6), 358–363. https://doi.org/10.1130/L67.1

Cohen, A., McGlue, M., Ellis, G., Zani, H., Swarzenski, P., Assine, M., & Silva, A. (2015). Lake formation, characteristics, and evolution in retroarc deposystems: A synthesis of the modern Andean orogen and its associated basins. Memoir of the Geological Society of America, 212, 309–335. https://doi.org/10.1130/2015.1212(16)

Cordani, U. G., Teixeira, W., Tassinari, C. C. G., Coutinho, J. M. V., & Ruiz, A. S. (2010). The Rio Apa Craton in Mato Grosso do Sul (Brazil) and northern Paraguay: Geochronological evolution, correlations and tectonic implications for Rodinia and Gondwana. American Journal of Science, 310(9), 981–1023. https://doi.org/10.2475/09.2010.09

Davaud, E., & Girardclos, S. (2001). Recent freshwater ooids and oncoids from western Lake Geneva (Switzerland): Indications of a common organically mediated origin. Journal of Sedimentary Research, 71(3), 423–429. https://doi.org/10.1306/2DC40950-0E47-11D7-8643000102C1865D

DeCelles, P. G., & Giles, K. A. (1996). Foreland basin systems. Basin Research, 8(2), 105–123. https://doi.org/10.1046/j.1365-2117.1996.01491.x

Decelles, P. G., & Hertel, F. (1989). Petrology of fluvial sands from the Amazonian foreland basin, Peru and Bolivia. GSA Bulletin, 101(12), 1552–1562. https://doi.org/10.1130/0016-7606(1989)101%3C1552:POFSFT%3E2.3.CO;2

Deckers, J., Nachtergaele, F., & Spaargaren, O. (2003). Tropical soils in the classification systems of USDA, FAO and WRB. Evolution of Tropical Soil Science: Past and Future: Workshop Brussels, 6 March 2002, 79–94.

Dias, F. L., Assumpção, M., Facincani, E. M., França, G. S., Assine, M. L., Paranhos Filho, A. C., & Gamarra, R. M. (2016). The 2009 earthquake, magnitude mb 4.8, in the Pantanal Wetlands,

west-central Brazil. Anais Da Academia Brasileira de Ciências, 88, 1253–1264. https://doi.org/10.1590/201620140507

Dickinson, W. R. (1985). Interpreting provenance relations from detrital modes of sandstones. In G. G. Zuffa (Ed.), Provenance of Arenites (pp. 333–361). Springer Netherlands. https://doi.org/10.1007/978-94-017-2809-6_15

Dickinson, W. R., Beard, L. S., Brakenridge, G. R., Erjavec, J. L., Ferguson, R. C., Inman, K. F., Knepp, R. A., Lindberg, F. A., & Ryberg, P. T. (1983). Provenance of North American Phanerozoic sandstones in relation to tectonic setting. GSA Bulletin, 94(2), 222–235. https://doi.org/10.1130/0016-7606(1983)94<222:PONAPS>2.0.CO;2

Faleiros, F. M., Pavan, M., Remédio, M. J., Rodrigues, J. B., Almeida, V. V., Caltabeloti, F. P., Pinto, L. G. R., Oliveira, A. A., Pinto de Azevedo, E. J., & Costa, V. S. (2016). Zircon U–Pb ages of rocks from the Rio Apa Cratonic Terrane (Mato Grosso do Sul, Brazil): New insights for its connection with the Amazonian Craton in pre-Gondwana times. Gondwana Research, 34, 187–204. https://doi.org/10.1016/j.gr.2015.02.018

Fantin-Cruz, I., de Oliveira, M. D., Campos, J. A., de Campos, M. M., de Souza Ribeiro, L., Mingoti, R., de Souza, M. L., Pedrollo, O., & Hamilton, S. K. (2020). Further development of small hydropower facilities will significantly reduce sediment transport to the Pantanal wetland of Brazil. Frontiers in Environmental Science, 8, 577748. https://doi.org/10.3389/fenvs.2020.577748

FAO. (1970). Soil map of the world IV. FAO-UNESCO (approx.) 1:5,000,000, Rome.

Fernandes, L. A., & Magalhães Ribeiro, C. M. (2015). Evolution and palaeoenvironment of the Bauru Basin (Upper Cretaceous, Brazil). Journal of South American Earth Sciences, 61, 71–90. https://doi.org/10.1016/j.jsames.2014.11.007

Fick, S. E., & Hijmans, R. J. (2017). WorldClim 2: new 1-km spatial resolution climate surfaces for global land areas. International Journal of Climatology, 37(12), 4302–4315. https://doi.org/10.1002/joc.5086

Garzanti, E. (2019). Petrographic classification of sand and sandstone. Earth-Science Reviews, 192, 545–563. https://doi.org/10.1016/j.earscirev.2018.12.014

Garzanti, E., Andò, S., & Vezzoli, G. (2008). Settling equivalence of detrital minerals and grain-size dependence of sediment composition. Earth and Planetary Science Letters, 273(1), 138–151. https://doi.org/10.1016/j.epsl.2008.06.020

Garzanti, E., Andò, S., & Vezzoli, G. (2009). Grain-size dependence of sediment composition and environmental bias in provenance studies. Earth and Planetary Science Letters, 277(3), 422–432. https://doi.org/10.1016/j.epsl.2008.11.007

Garzanti, E., Andò, S., Vezzoli, G., Ali Abdel Megid, A., & El Kammar, A. (2006). Petrology of Nile River sands (Ethiopia and Sudan): Sediment budgets and erosion patterns. Earth and Planetary Science Letters, 252(3), 327–341. https://doi.org/10.1016/j.epsl.2006.10.001

Garzanti, E., Padoan, M., Andò, S., Resentini, A., Vezzoli, G., & Lustrino, M. (2013). Weathering and relative durability of detrital minerals in equatorial climate: Sand petrology and geochemistry in the East African Rift. The Journal of Geology, 121(6), 547–580. https://doi.org/10.1086/673259

Garzanti, E., Vermeesch, P., Padoan, M., Resentini, A., Vezzoli, G., & Andò, S. (2014). Provenance of passive-margin sand (Southern Africa). The Journal of Geology, 122(1), 17–42. https://doi.org/10.1086/674803

Garzanti, E., Andò, S., Padoan, M., Vezzoli, G., & El Kammar, A. (2015). The modern Nile sediment system: Processes and products. Quaternary Science Reviews, 130, 9–56. https://doi.org/10.1016/j.quascirev.2015.07.011

Garzanti, E., Capaldi, T., Tripaldi, A., Zárate, M., Limonta, M., & Vezzoli, G. (2022). Andean retroarc-basin dune fields and Pampean Sand Sea (Argentina): Provenance and drainage changes driven by tectonics and climate. Earth-Science Reviews, 231, 104077. https://doi.org/10.1016/j.earscirev.2022.104077

Garzanti, E., Capaldi, T., Vezzoli, G., Limonta, M., & Sosa, N. (2021a). Transcontinental retroarc sediment routing controlled by subduction geometry and climate change (Central and Southern Andes, Argentina). Basin Research, 33(6), 3406–3437. https://doi.org/10.1111/bre.12607

Garzanti, E., Limonta, M., Vezzoli, G., & Sosa, N. (2021b). From Patagonia to Río de la Plata: Multistep long-distance littoral transport of Andean volcaniclastic sand along the Argentine passive margin. Sedimentology, 68(7), 3357–3384. https://doi.org/10.1111/sed.12902

Garzanti, E., He, J., Barbarano, M., Resentini, A., Li, C., Yang, L., Yang, S., & Wang, H. (2021c). Provenance versus weathering control on sediment composition in tropical monsoonal climate (South China) - 2. Sand petrology and heavy minerals. Chemical Geology, 564, 119997. https://doi.org/10.1016/j.chemgeo.2020.119997

Geno, K. R., & Chafetz, H. S. (1982). Petrology of Quaternary fluvial low-magnesian calcite coated grains from central Texas. Journal of Sedimentary Research, 52(3), 833–842. https://doi.org/10.1306/212F8067-2B24-11D7-8648000102C1865D

Gleyzer, A., Denisyuk, M., Rimmer, A., & Salingar, Y. (2004). A fast recursive GIS algorithm for computing Strahler stream order in braided and nonbraided networks. JAWRA Journal of the American Water Resources Association, 40(4), 937–946. https://doi.org/10.1111/j.1752-1688.2004.tb01057.x

Godoy, J. M., Padovani, C. R., Guimarães, J. R. D., Pereira, J. C. A., Vieira, L. M., Carvalho, Z. L., & Galdino, S. (2002). Evaluation of the siltation of River Taquari, Pantanal, Brazil, through 210Pb geochronology of floodplain lake sediments. Journal of the Brazilian Chemical Society, 13, 71–77. https://doi.org/10.1590/S0103-50532002000100011

Grossman, R. B. (1983). Chapter 2 Entisols. In L. P. Wilding, N. E. Smeck, & G. F. Hall (Eds.), Developments in Soil Science (Vol. 11, pp. 55–90). Elsevier. https://doi.org/10.1016/S0166-2481(08)70613-5

Hatzenbühler, D., Caracciolo, L., Weltje, G. J., Piraquive, A., & Regelous, M. (2022). Lithologic, geomorphic, and climatic controls on sand generation from volcanic rocks in the Sierra Nevada de Santa Marta massif (NE Colombia). Sedimentary Geology, 429, 106076. https://doi.org/10.1016/j.sedgeo.2021.106076

Heins, W. A. (1993). Source rock texture versus climate and topography as controls on the composition of modern, plutoniclastic sand. In M. J. Johnsson & A. Basu (Eds.), Processes Controlling the Composition of Clastic Sediments (Vol. 284, p. 135-146). Geological Society of America. https://doi.org/10.1130/SPE284-p135

Heins, W., & Kairo, S. (2007). Predicting sand character with integrated genetic analysis. In Special Paper of the Geological Society of America (Vol. 420, pp. 345–379). https://doi.org/10.1130/2006.2420(20)

Horbe, A. M. C., Motta, M. B., de Almeida, C. M., Dantas, E. L., & Vieira, L. C. (2013). Provenance of Pliocene and

recent sedimentary deposits in western Amazônia, Brazil: Consequences for the paleodrainage of the Solimões-Amazonas River. Sedimentary Geology, 296, 9–20. https://doi.org/10.1016/j.sedgeo.2013.07.007

Horton, B. K. (2022). Unconformity development in retroarc foreland basins: implications for the geodynamics of Andean-type margins. Journal of the Geological Society, 179(3), jgs2020-263. https://doi.org/10.1144/jgs2020-263

Horton, B. K., & DeCelles, P. G. (1997). The modern foreland basin system adjacent to the Central Andes. Geology, 25(10), 895–898. https://doi.org/10.1130/0091-7613(1997)025%3C0895:TMFBSA%3E2.3.CO;2

Islam, Md. R., Stuart, R., Risto, A., & Vesa, P. (2002). Mineralogical changes during intense chemical weathering of sedimentary rocks in Bangladesh. Journal of Asian Earth Sciences, 20(8), 889–901. https://doi.org/10.1016/S1367-9120(01)00078-5

Ivory, S. J., McGlue, M. M., Spera, S., Silva, A., & Bergier, I. (2019). Vegetation, rainfall, and pulsing hydrology in the Pantanal, the world's largest tropical wetland. Environmental Research Letters, 14, 124017. https://doi.org/10.1088/1748-9326/ab4ffe

Johnson, J. I., Sharman, G. R., Szymanski, E., & Huang, X. (2022). Machine learning applied to a modern-Pleistocene petrographic data set: The Global Prediction of Sand Modal Composition (GloPrSM) Model. Journal of Geophysical Research: Earth Surface, 127(7), e2022JF006595. https://doi.org/10.1029/2022JF006595

Johnsson, M. J. (1990). Tectonic versus chemical-weathering controls on the composition of fluvial sands in tropical environments. Sedimentology, 37(4), 713–726. https://doi.org/10.1111/j.1365-3091.1990.tb00630.x

Johnsson, M. J., Stallard, R. F., & Lundberg, N. (1991). Controls on the composition of fluvial sands from a tropical weathering environment: Sands of the Orinoco River drainage basin, Venezuela and Colombia. GSA Bulletin, 103(12), 1622–1647. https://doi.org/10.1130/0016-7606(1991)103%3C1622:COTCOF%3E2.3.CO;2

Jonell, T. N., Clift, P. D., Hoang, L. V., Hoang, T., Carter, A., Wittmann, H., Böning, P., Pahnke, K., & Rittenour, T. (2017). Controls on erosion patterns and sediment transport in a monsoonal, tectonically quiescent drainage, Song Gianh, central Vietnam. Basin Research, 29(S1), 659–683. https://doi.org/10.1111/bre.12199

Junk, W. J., da Cunha, C. N., Wantzen, K. M., Petermann, P., Strüssmann, C., Marques, M. I., & Adis, J. (2006). Biodiversity and its conservation in the Pantanal of Mato Grosso, Brazil. Aquatic Sciences, 68(3), 278–309. https://doi.org/10.1007/s00027-006-0851-4

Komar, P. D. (1987). Selective grain entrainment by a current from a bed of mixed sizes; a reanalysis. Journal of Sedimentary Research, 57(2), 203–211. https://doi.org/10.1306/212F8AE4-2B24-11D7-8648000102C1865D

Kroonenberg, S. (1992). Effects of provenance, sorting and weathering on the geochemistry of fluvial sands from different tectonic and climatic environments. In Proceedings of the 29th International Geological Congress Part A (pp. 69–81).

Kuerten, S., & Stevaux, J. C. (2021). Megaleques das bacias sedimentares do Chaco e Pantanal: uma revisão comparada. Revista Brasileira de Geomorfologia, 22(3), 532-558. https://doi.org/10.20502/rbg.v22i3.1886

Latrubesse, E. M., Stevaux, J. C., Cremon, E. H., May, J.-H., Tatumi, S. H., Hurtado, M. A., Bezada, M., & Argollo, J. B. (2012). Late Quaternary megafans, fans and fluvio-aeolian interactions in the Bolivian Chaco, Tropical South America. Palaeogeography, Palaeoclimatology, Palaeoecology, 356–357, 75–88. https://doi.org/10.1016/j.palaeo.2012.04.003

Louzada, R. O., Bergier, I., & Assine, M. L. (2020). Landscape changes in avulsive river systems: Case study of Taquari River on Brazilian Pantanal wetlands. Science of The Total Environment, 723, 138067. https://doi.org/10.1016/j.scitotenv.2020.138067

Louzada, R. O., Bergier, I., Roque, F. O., McGlue, M. M., Silva, A., & Assine, M. L. (2021). Avulsions drive ecosystem services and economic changes in the Brazilian Pantanal wetlands. Current Research in Environmental Sustainability, 3, 100057. https://doi.org/10.1016/j.crsust.2021.100057

Marengo, J., Sampaio, G., & Alves, L. (2015). Climate change scenarios in the Pantanal. In Handbook of Environmental Chemistry (pp. 227–238). https://doi.org/10.1007/698_2015_357

McGlue, M. M., Guerreiro, R. L., Bergier, I., Silva, A., Pupim, F. do N., Oberc, V., & Assine, M. L. (2017). Holocene stratigraphic evolution of saline lakes in Nhecolândia, southern Pantanal wetlands (Brazil). Quaternary Research, 88(3), 472–490. https://doi.org/10.1017/qua.2017.57

McGlue, M. M., Silva, A., Corradini, F. A., Zani, H., Trees, M. A., Ellis, G. S., Parolin, M., Swarzenski, P. W., Cohen, A. S., & Assine, M. L. (2011). Limnogeology in Brazil's "forgotten wilderness": a synthesis from the large floodplain lakes of the Pantanal. Journal of Paleolimnology, 46(2), 273–289. https://doi.org/10.1007/s10933-011-9538-5

McGlue, M. M., Smith, P. H., Zani, H., Silva, A., Carrapa, B., Cohen, A. S., & Pepper, M. B. (2016). An integrated sedimentary systems analysis of the Río Bermejo (Argentina): Megafan character in the overfilled southern Chaco foreland basin. Journal of Sedimentary Research, 86(12), 1359–1377. https://doi.org/10.2110/jsr.2016.82

Merino, E. R., & Assine, M. L. (2020). Hidden in plain sight: How finding a lake in the Brazilian Pantanal improves understanding of wetland hydrogeomorphology. Earth Surface Processes and Landforms, 45(2), 440–458. https://doi.org/10.1002/esp.4745

Miller, K. L., Szabó, T., Jerolmack, D. J., & Domokos, G. (2014). Quantifying the significance of abrasion and selective transport for downstream fluvial grain size evolution. Journal of Geophysical Research: Earth Surface, 119(11), 2412–2429. https://doi.org/10.1002/2014JF003156

Novello, V. F., Cruz, F. W., Vuille, M., Stríkis, N. M., Edwards, R. L., Cheng, H., Emerick, S., de Paula, M. S., Li, X., Barreto, E. de S., Karmann, I., & Santos, R. V. (2017). A high-resolution history of the South American Monsoon from Last Glacial Maximum to the Holocene. Scientific Reports, 7(1), 44267. https://doi.org/10.1038/srep44267

Odom, I. E. (1975). Feldspar-grain size relations in Cambrian arenites, upper Mississippi Valley. Journal of Sedimentary Research, 45(3), 636–650. https://doi.org/10.1306/212F6E01-2B24-11D7-8648000102C1865D

Olson, D. M., Dinerstein, E., Wikramanayake, E. D., Burgess, N. D., Powell, G. V. N., Underwood, E. C., D'amico, J. A., Itoua, I., Strand, H. E., Morrison, J. C., Loucks, C. J., Allnutt, T. F., Ricketts, T. H., Kura, Y., Lamoreux, J. F., Wettengel, W. W., Hedao, P., & Kassem, K. R. (2001). Terrestrial Ecoregions of the World: A New Map of Life on Earth: A new global map of terrestrial ecoregions provides an innovative tool for conserving biodiversity. BioScience, 51(11), 933–938. https://doi.org/10.1641/0006-3568(2001)051[0933:TEOTWA]2.0.CO;2

Oste, J. T. F., Rodríguez-Berriguete, Á., & Dal' Bó, P. F. (2021). Depositional and environmental controlling factors on the genesis of Quaternary tufa deposits from Bonito region,

Central-West Brazil. Sedimentary Geology, 413, 105824. https://doi.org/10.1016/j.sedgeo.2020.105824

Pacton, M., Ariztegui, D., Wacey, D., Kilburn, M. R., Rollion-Bard, C., Farah, R., & Vasconcelos, C. (2012). Going nano: A new step toward understanding the processes governing freshwater ooid formation. Geology, 40(6), 547–550. https://doi.org/10.1130/G32846.1

Papa, C. del, Payrola, P., Pingel, H., Hongn, F., Campo, M. D., Sobel, E. R., Lapiana, A., Cottle, J., Glodny, J., & Strecker, M. R. (2021). Stratigraphic response to fragmentation of the Miocene Andean foreland basin, NW Argentina. Basin Research, 33(6), 2914–2937. https://doi.org/10.1111/bre.12589

Paz, A. R., Bravo, J. M., Allasia, D., Collischonn, W., & Tucci, C. E. M. (2010). Large-scale hydrodynamic modeling of a complex river network and floodplains. Journal of Hydrologic Engineering, 15(2), 152–165. https://doi.org/10.1061/(ASCE)HE.1943-5584.0000162

Pettijohn, F. J. (1954). Classification of sandstones. The Journal of Geology, 62(4), 360–365. https://doi.org/10.1086/626172

Pupim, F. do N., Assine, M. L., & Sawakuchi, A. O. (2017). Late Quaternary Cuiabá megafan, Brazilian Pantanal: Channel patterns and paleoenvironmental changes. Quaternary International, 438, 108–125. https://doi.org/10.1016/j.quaint.2017.01.013

RadamBrasil, P. (1982). Projeto Radambrasil: levantamento de recursos naturais. Ministério das Minas e Energia. Secretária Geral. Rio de Janeiro.

Ribeiro, F. B., Roque, A., Boggiani, P. C., & Flexor, J.-M. (2001). Uranium and thorium series disequilibrium in quaternary carbonate deposits from the Serra da Bodoquena and Pantanal do Miranda, Mato Grosso do Sul State, central Brazil. Applied Radiation and Isotopes, 54(1), 153–173. https://doi.org/10.1016/S0969-8043(99)00265-1

Rivadeneyra-Vera, C., Bianchi, M., Assumpção, M., Cedraz, V., Julià, J., Rodríguez, M., Sánchez, L., Sánchez, G., Lopez-Murua, L., Fernandez, G., Fugarazzo, R., & Team T.B.P. (2019). An updated crustal thickness map of central South America based on receiver function measurements in the region of the Chaco, Pantanal, and Paraná Basins, southwestern Brazil. Journal of Geophysical Research: Solid Earth, 124(8), 8491–8505. https://doi.org/10.1029/2018JB016811

Rizzotto, G., & Hartmann, L. (2012). Geological and geochemical evolution of the Trincheira Complex, a Mesoproterozoic ophiolite in the southwestern Amazon craton, Brazil. Lithos, 148, 277–295. https://doi.org/10.1016/j.lithos.2012.05.027

Rodrigues, A. A., Macedo, M. N., Silvério, D. V., Maracahipes, L., Coe, M. T., Brando, P. M., Shimbo, J. Z., Rajão, R., Soares-Filho, B., & Bustamante, M. M. C. (2022). Cerrado deforestation threatens regional climate and water availability for agriculture and ecosystems. Global Change Biology, 28(22), 6807–6822. https://doi.org/10.1111/gcb.16386

Savage, K. M., & Potter, P. E. (1991). Petrology of modern sands of the Rios Guaviare and Inirida, southern Colombia: Tropical climate and sand composition. The Journal of Geology, 99(2), 289–298. https://doi.org/10.1086/629489

Schiavo, J. A., Pereira, M. G., Miranda, L. P. M. de, Dias Neto, A. H., & Fontana, A. (2010). Caracterização e classificação de solos desenvolvidos de arenitos da formação Aquidauana-MS. Revista Brasileira de Ciência do Solo, 34, 881–889. https://doi.org/10.1590/S0100-06832010000300029

Shirzad, T., Assumpcao, M., & Bianchi, M. (2020). Ambient seismic noise tomography in west-central and Southern Brazil, characterizing the crustal structure of the Chaco-Paraná, Pantanal and Paraná basins. Geophysical Journal International, 220(3), 2074–2085. https://doi.org/10.1093/gji/ggz548

Sileshi, G. W., Kihara, J., Tamene, L., Vanlauwe, B., Phiri, E., & Jama, B. (2022). Unravelling causes of poor crop response to applied N and P fertilizers on African soils. Experimental Agriculture, 58, 1-17. https://doi.org/10.1017/S0014479721000247

Silva, M. B., Anjos, L. H. C. dos, Pereira, M. G., Schiavo, J. A., Cooper, M., & Cavassani, R. de S. (2017). Soils in the karst landscape of Bodoquena plateau in cerrado region of Brazil. Catena, 154, 107–117. https://doi.org/10.1016/j.catena.2017.02.022

Strey, S., Boy, J., Strey, R., Weber, O., & Guggenberger, G. (2016). Response of soil organic carbon to land-use change in central Brazil: A large-scale comparison of Ferralsols and Acrisols. Plant and Soil, 408(1), 327–342. https://doi.org/10.1007/s11104-016-2901-6

Suttner, L. J., & Dutta, P. K. (1986). Alluvial sandstone composition and paleoclimate; I, Framework mineralogy. Journal of Sedimentary Research, 56(3), 329–345. https://doi.org/10.1306/212F8909-2B24-11D7-8648000102C1865D

Terra, F. S., Demattê, J. A. M., & Viscarra Rossel, R. A. (2018). Proximal spectral sensing in pedological assessments: vis–NIR spectra for soil classification based on weathering and pedogenesis. Geoderma, 318, 123–136. https://doi.org/10.1016/j.geoderma.2017.10.053

Tineo, D. E. (2020). Facies model of a sedimentary record for a Pantanal-like inland wetland. Sedimentology, 67(7), 3683–3717. https://doi.org/10.1111/sed.12766

USGS. (1996). Global 30 Arc-Second Elevation (GTOPO30). https://doi.org/10.5066/F7DF6PQS

Ussami, N., Shiraiwa, S., & Dominguez, J. M. L. (1999). Basement reactivation in a sub-Andean foreland flexural bulge: The Pantanal wetland, SW Brazil. Tectonics, 18(1), 25–39. https://doi.org/10.1029/1998TC900004

Verdin, K. L. (2017). Hydrologic derivatives for modeling and analysis—A new global high-resolution database. In Data Series (No. 1053). U.S. Geological Survey. https://doi.org/10.3133/ds1053

Vezzoli, G., Ghielmi, G., Mondaca, G., Resentini, A., Villarroel, E. K., Padoan, M., & Gentile, P. (2013). Quantifying modern erosion rates and river-sediment contamination in the Bolivian Andes. Journal of South American Earth Sciences, 45, 42–55. https://doi.org/10.1016/j.jsames.2013.02.001

Warren, L., Quaglio, F., Simoes, M., Freitas, B., Assine, M., & Riccomini, C. (2015). Underneath the Pantanal wetland: A deep-time history of Gondwana assembly, climate change, and the dawn of metazoan life. In Handbook of Environmental Chemistry. https://doi.org/10.1007/698_2014_326

Weissmann, G. S., Hartley, A. J., Scuderi, L. A., Nichols, G. J., Owen, A., Wright, S., Felicia, A. L., Holland, F., & Anaya, F. M. L. (2015). Fluvial geomorphic elements in modern sedimentary basins and their potential preservation in the rock record: A review. Geomorphology, 250, 187–219. https://doi.org/10.1016/j.geomorph.2015.09.005

Wu, F.-T., & Caetano-Chang, M. R. (1992). Estudo mineralógico dos arenitos das formações Pirambóia e Botucatu no Centro-Leste do Estado de São Paulo. Revista do Instituto Geológico, 13(1), 58-68. https://doi.org/10.5935/0100-929X.19920004

Zani, H., Assine, M. L., & McGlue, M. M. (2012). Remote sensing analysis of depositional landforms in alluvial settings: Method development and application to the Taquari megafan, Pantanal (Brazil). Geomorphology, 161–162, 82–92. https://doi.org/10.1016/j.geomorph.2012.04.003

How to cite: Lo, E. L., Silva, A., Kuerten, S., Louzada, R. O., Rasbold, G. G., & McGlue, M. M. (2023). Source-to-sink controls on modern fluvial sands in the Pantanal back-bulge basin (Brazil). Sedimentologika, 1(1), 1-18. https://doi.org/10.57035/journals/sdk.2023.e11.1152